Accepted Manuscript

Effects on tubulin polymerization and down-regulation of c-Myc, hTERT and VEGF genes by colchicine haloacetyl and haloaroyl derivatives

Ana Marzo-Mas, Eva Falomir, Juan Murga, Miguel Carda, J. Alberto Marco

PII: S0223-5234(18)30254-X

DOI: 10.1016/j.ejmech.2018.03.019

Reference: EJMECH 10284

To appear in: *European Journal of Medicinal Chemistry*

Received Date: 21 November 2017

Revised Date: 1 March 2018

Accepted Date: 5 March 2018

Please cite this article as: A. Marzo-Mas, E. Falomir, J. Murga, M. Carda, J.A. Marco, Effects on tubulin polymerization and down-regulation of c-Myc, hTERT and VEGF genes by colchicine haloacetyl and haloaroyl derivatives, *European Journal of Medicinal Chemistry* (2018), doi: 10.1016/j.ejmech.2018.03.019.

Effects on tubulin polymerization and down-regulation of c-Myc, hTERT and VEGF genes by colchicine haloacetyl and haloaroyl derivatives

Ana Marzo-Mas, Eva Falomir, Juan Murga, Miguel Carda and J. Alberto Marco

Graphical Abstract

Several *N*-acyl colchicine analogues have been synthesized and their cytotoxicity, their effects on inhibition of tubulin polymerization and cell cycle have been evaluated. Moreover their capacity to downregulate some oncogenes at nontoxic dosis have been evaluated. The haloaroyl moiety enhances oncogene down-regulation effect as regards colchicine itself. Outstanding results for *m*-chlorobenzoylderivative **14** were obtained as this derivative is able to decrease the expression of oncogenes involved in tumor aggressiveness at concentrations in which there is no antimitotic effect.

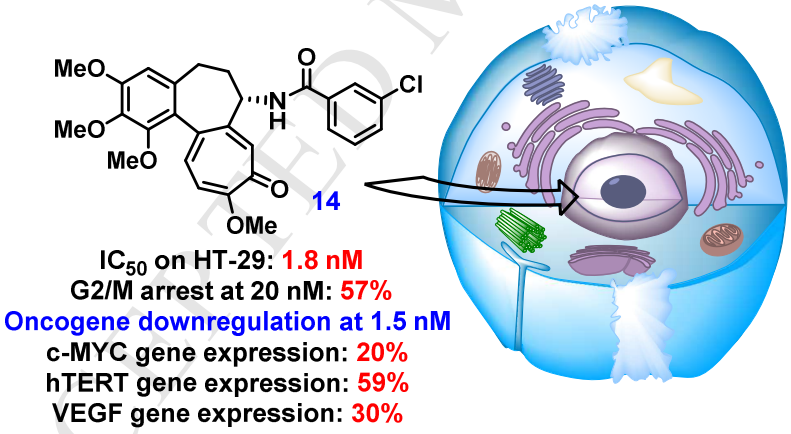

Manuscript draft

Title: Effects on tubulin polymerization and down-regulation of c-Myc, hTERT and VEGF genes by colchicine haloacetyl and haloaroyl derivatives

Article type: Original paper

Keywords: tubulin, colchicine, microtubules, polymerization, cell cycle, c-Myc, hTERT, VEGF, oncogene.

Abstract:

Several colchicine analogues in which the *N*-acetyl residue has been replaced by haloacetyl, cyclohexylacetyl, phenylacetyl and various aroyl moieties have been synthesized. The cytotoxic activities of the synthesized compounds have been measured on three tumor cell lines (HT-29, MCF-7 and A549) and on one non-tumor cell line (HEK-293). These compounds exhibit high antiproliferative activities at the nanomolar level, in many cases with a higher potency than colchicine itself. Some of the compounds, particularly the haloacetyl derivatives, inhibit the polymerization of tubulin in a similar manner as colchicine. As regards the cell cycle, the most active compounds are the chlorobenzoyl and bromobenzoyl derivatives, which cause cell cycle arrest at the G2/M phase when tested at 20 nM, and the bromoacetyl derivative, which arrests the cell cycle at 15 nM. In addition, these colchicine derivatives have shown fairly active downregulating the expression of the c-*Myc*, *hTERT* and *VEGF* genes, as well as VEGF protein secretion, at very low concentrations.

EFFECTS ON TUBULIN POLYMERIZATION AND DOWN-REGULATION OF C-MYC, HTERT AND VEGF GENES BY COLCHICINE HALOACETYL AND HALOAROYL DERIVATIVES

Ana Marzo-Mas,[a] *Eva Falomir,**[a] *Juan Murga,**[a] *Miguel Carda*[a] *and J. Alberto Marco*[b]

[a]Depart. de Q. Inorgánica y Orgánica, Univ. Jaume I, E-12071 Castellón, Spain
[b]Depart. de Q. Orgánica, Univ. de Valencia, E-46100 Burjassot, Valencia, Spain

*Authors to whom correspondence should be addressed. E-Mail address: jmurga@uji.es, efalomir@uji.es

ABSTRACT

Several colchicine analogues in which the *N*-acetyl residue has been replaced by haloacetyl, cyclohexylacetyl, phenylacetyl and various aroyl moieties have been synthesized. The cytotoxic activities of the synthesized compounds have been measured on three tumor cell lines (HT-29, MCF-7 and A-549) and on one non-tumor cell line (HEK-293). These compounds exhibit high antiproliferative activities at the nanomolar level, in many cases with a higher potency than colchicine itself. Some of the compounds, particularly the haloacetyl derivatives, inhibit the polymerization of tubulin in a similar manner as colchicine. As regards the cell cycle, the most active compounds are the chlorobenzoyl and bromobenzoyl derivatives, which cause cell cycle arrest at the G2/M phase when tested at 20 nM, and the bromoacetyl derivative, which arrests the cell cycle at 15 nM. In addition, these colchicine derivatives have shown fairly active downregulating the expression of the c-*Myc*, *hTERT* and *VEGF* genes, as well as VEGF protein secretion, at very low concentrations.

KEYWORDS

tubulin, colchicine, microtubules, polymerization, cell cycle, *c-Myc*, *hTERT*, *VEGF*, oncogene.

1. Introduction

Colchicine is an alkaloid isolated from the poisonous plant meadow saffron *Colchicum autumnale* L. This compound has been used in the treatment of several inflammatory diseases such as gout, familial Mediterranean fever, pericarditis and Behçet's disease [1]. The primary mechanism of action of

this natural product involves disruption of the tubulin microtubules. In fact, colchicine was the first compound known to bind tubulin [2]. The microtubule disrupting action is responsible for the blockage of migration of neutrophils to the damaged tissue thereby inhibiting the inflammatory process. Some studies have revealed that the anti-inflammatory effect of colchicine may be mediated not only by microtubule disruption but also by changes at transcriptional level. In this sense, it has been found that colchicine was able to supress many genes related not only to the inflammation process but also to cell cycle regulation. The handicap was that the concentration of natural product required to exert this transcriptional regulation was higher than the therapeutic dose [3].

Colchicine is not clinically used in cancer treatments due to its relatively narrow therapeutic index. Although a significant percentage of patients report adverse effects at daily doses when colchicine is administered to treat the above mentioned diseases, colchicine may be administered to tolerant patients for long periods of time without any side effect [4].

Many efforts have been made to find more effective and less toxic colchicine derivatives by means of modifying its structure [5]. As a matter of fact, some derivatives of colchicine, such as thiocolchicoside (Neoflax™, Muscoril™) are being used as anti-inflammatory and analgesic drugs.

In this sense, we have designed, synthesized and studied some hybrid molecules with a colchicine moiety and a pironetin analogue fragment. We found that, in addition to binding to tubulin, these compounds were able to downregulate the expression of the *VEGF*, *hTERT* and *c-Myc* genes. These three genes are of paramount importance in the cancer generation process. Our results pointed to the colchicine fragment being responsible for the observed biological activities, although high doses were required (50 nM-15 μM). [6]

It has been reported that deregulation of *c-Myc* plays a major role in the carcinogenesis of human malignancies and very often correlates with upregulation of *VEGF* and *hTERT* expression [7]. It has also been determined that *c-Myc* upregulation is associated with low prognosis and that inactivation of *c-Myc* or downstream targets of this one, might provide important therapeutic strategies [8].

In order to expand our research on colchicine derivatives with potential utility in cancer therapy not only as anti-mitotic compounds but also as downregulators of some oncogenes, we decided to investigate the influence of the *N*-acetyl group of the natural product in this latter activity. The purpose was to get colchicine derivatives with enhanced anticancer properties and lower toxicity. Thus, we designed a set of *N*-acyl derivatives (see Figure 1) that would let us observe the influence of the electronic and steric nature of this residue in colchicine derivatives. In this family of colchicine

derivatives we have included *N*-haloacetyl **1**-**4**, *N*-cyclohexylacetyl **5**, *N*-phenylacetyl **6**, and *N*-aroyl moieties **7**-**18**.

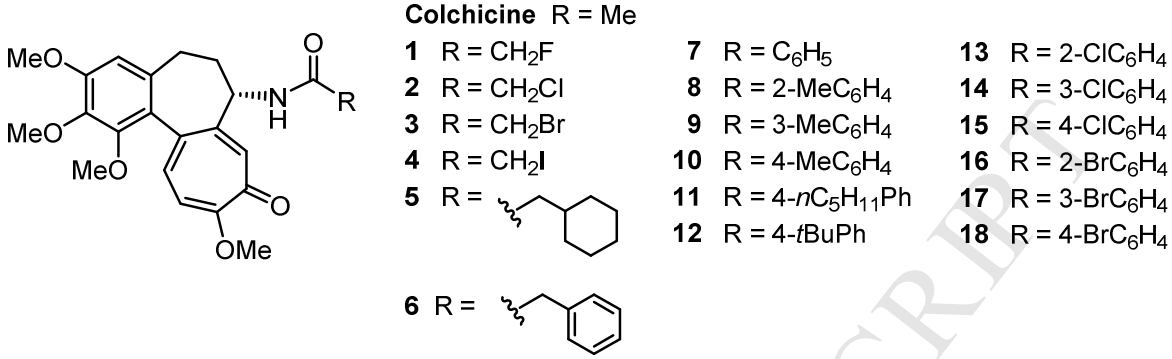

Figure 1. Structure of the colchicine analogues investigated in this study

2. Results and discussion

2.1. Preliminary docking studies

Before starting the synthesis and biological evaluation of these colchicine derivatives, we carried out docking studies in order to find out whether these derivatives preserved the ability to bind to tubulin at/or near the colchicine binding site, in a similar conformation to the natural product. Thus, Autodock 4.2 [9] was used to perfom molecular docking calculations and the crystal structure of αβ tubulin (PDB ID 1SA0) [10] was employed as a template. Figure 2 (Panel A) shows a superimposition of DAMA-colchicine [*N*-deacetyl-*N*-(2- mercaptoacetyl)colchicine], obtained from the PDB ID 1SA0 over the structures of the haloacetyl derivatives **1**-**4**. These docking experiments suggest that derivatives **1**-**4** exhibit conformations very close to that of DAMA-colchicine. As an example, panel B shows the location of floruoacetyl derivative **1** at the β-tubulin binding site. The docking score, based in free energy of binding, is included in the Supplementary Information (Table SI-1). Structures **1**-**4** show the same interactions that the crystallized structure of DAMA-colchicine (see 2D interactions in Figures SI-1, SI-2 and SI-3 in Supplementary Information).

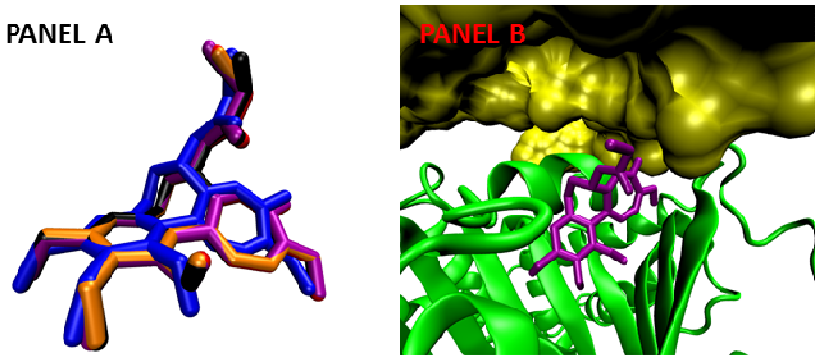

Figure 2. Panel A corresponds to the superimposition of the structures of **1** (black), **2** (orange), **3** (red) and **4** (purple) on the co-crystallized DAMA-colchicine (blue) at the colchicine binding site. Panel B corresponds to the structure of fluoroacetyl derivative **1** at the colchicine binding site. The α- and β-tubulin subunits are coloured in yellow and green, respectively.

As regards the aroyl derivatives, we selected the bromo derivatives **16-18** to perform docking calculations. Figure 3 (Panel A) shows a superimposition of DAMA-colchicine over the structures of these compounds.

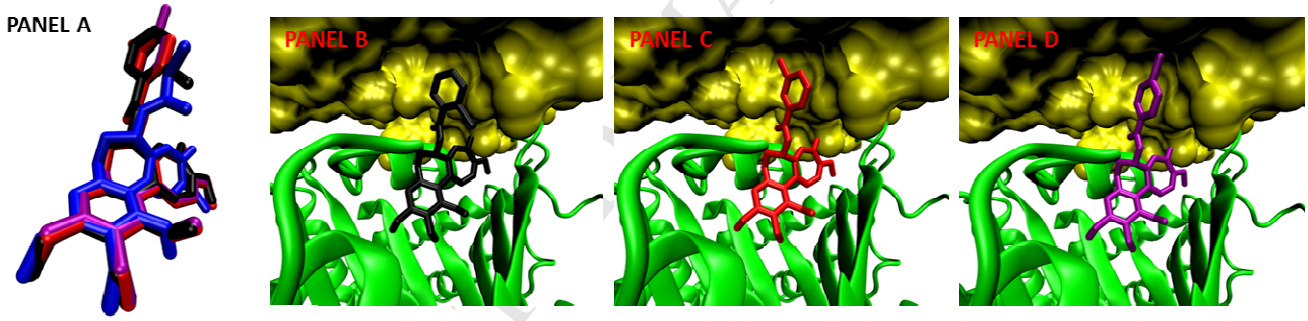

Figure 3. Panel A corresponds to the superimposition of the structures of **16** (black), **17** (red) and **18** (purple) on the co-crystallized DAMA-colchicine (blue) at the colchicine binding site. Panel B, C and D correspond, respectively, to the structures of **16**, **17** and **18** at the colchicine binding site. The α- and β-tubulin subunits are coloured in yellow and green, respectively.

As shown in Figure 3 (panels B, C and D), bromoaroyl derivatives **16-18** bind to the binding site of the colchicine at the β-tubulin domain in a very close conformation to that of DAMA-colchicine, with the bromoaroyl unit pointing towards a hydrophobic cavity of the adjacent alpha subunit of tubulin. The bromoaroyl derivatives **16-18** showed lower binding energy when compared with compounds **1-4**. An extra hydrogen bond interaction between αAsn101 and the carbonyl group of acyl residue is formed (see 2D interactions in Figures SI-4 and SI-5 in Supplementary Information). Also, the aromatic ring of

bromoaryl unit shows an interaction with αAla180. These extra interacions could explain the lower binding energy of compounds **16**-**18**. According to the docking results, all these derivatives retain the ability to bind to tubulin at the colchicine binding site.

2.2. Chemistry

The trifluoroacetate salt of *N*-deacetyl colchicine **19** [11] was used as the starting material to prepare the *N*-acyl derivatives **1**-**18** as depicted in Scheme 1. Treatment of **19** with the corresponding carboxylic acid in the presence of DCC and DMAP afforded compounds **1**-**18** with fair yields. Details about the precise reaction conditions and yields are indicated in the Experimental Part together with complete spectral data (graphical spectra are provided in the Supporting Information) [12].

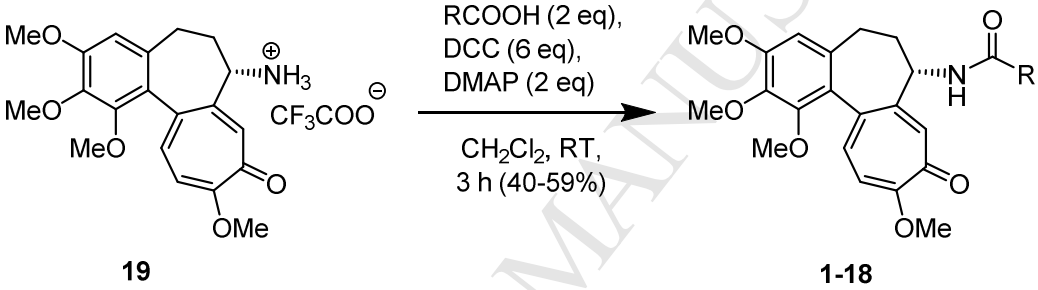

Scheme 1. Synthesis of colchicine derivatives **1**-**18**.

2.3. Biological evaluation

2.3.1. Effects on the inhibition of cell proliferation

The MTT assay was used to measure the ability of compounds **1**-**19** to inhibit cell proliferation, expressed by means of their IC_{50} values towards the tumoral cell lines HT-29 (human colon adenocarcinoma), MCF-7 (breast adenocarcinoma) and A549 (human alveolar lung epithelial carcinoma cells), as well as towards the non-tumoral cell line HEK-293 (human embryonic kidney cells). The results were compared with those of colchicine and are depicted in Table 1 along with the calculated selectivity indexes SI_A (for HT-29 cell line), SI_B (for MCF-7 cell line) and SI_c (for A549 cell line), obtained by dividing the IC_{50} values of the non-tumoral cell line (HEK-293) by those of the corresponding tumoral cell line. The SI value is a parameter that helps to estimate the possible selectivity of compounds for cancer cells in relation to non-cancer cells. Thus, a higher SI index indicates a higher therapeutic safety margin.

Table 1. IC_{50} values (nM) of synthetic compounds **1-19** in cancer cell lines HT-29, MCF-7 and A549, and one non-cancer cell line HEK-293.[a]

Compound	HT-29	MCF-7	A549	HEK-293	SI_A[b]	SI_B[c]	SI_C[d]
Colchicine	50 ± 3	12 ± 7	12.2 ± 0.7	5 ± 1	0.1	0.4	0.4
1	4.7 ± 1.3	7.3 ± 1.2	7.83 ± 0.15	7.1 ± 0.5	1.5	1.0	0.9
2	4.6 ± 0.4	29 ± 1	12.3 ± 2.1	4.56 ± 0.08	1.0	0.2	0.4
3	13.7 ± 0.2	16.4 ± 0.3	26 ± 5	14.36 ± 1.06	1.0	0.9	0.6
4	10 ± 1	4.1 ± 0.8	31 ± 3	19 ± 1	1.9	4.6	0.6
5	8.7 ± 0.5	9 ± 2	19.4 ± 3.1	10.5 ± 0.9	1.2	1.2	0.5
6	2.84 ± 0.04	2.6 ± 0.9	2.8 ± 0.9	3.9 ± 0.7	1.4	1.5	1.4
7	8.1 ± 0.9	5 ± 2	10 ± 3	13 ± 5	1.6	2.6	1.3
8	5.7 ± 0.5	2.02 ± 0.04	2.0 ± 0.6	9.0 ± 1.2	1.6	4.5	4.5
9	2.23 ± 0.23	5.6 ± 1.5	8.7 ± 1.3	3.1 ± 0.9	1.4	0.6	0.4
10	9.0 ± 2.2	31 ± 8	8.8 ± 1.2	16.1 ± 0.6	1.8	0.5	1.8
11	4.2 ± 1.2	5.8 ± 1.8	1.27 ± 0.4	1.6 ± 0.4	0.4	0.3	1.3
12	32.7 ± 2.1	24 ± 4	36 ± 6	58 ± 11	1.8	2.4	1.6
13	2.3 ± 0.4	4.5 ± 0.6	13 ± 3	5.93 ± 0.06	2.6	1.3	0.5
14	1.8 ± 0.3	3.4 ± 0.6	3.1 ± 1.1	3.0 ± 0.3	1.7	0.9	1.0
15	1.79 ± 0.15	6.7 ± 0.4	6.6 ± 1.0	10.1 ± 2.4	5.6	1.5	1.5
16	5.8 ± 0.3	7.6 ± 1.9	13 ± 3	8.5 ± 2.8	1.5	1.1	0.7
17	0.56 ± 0.04	0.363 ± 0.013	14 ± 4	1.1 ± 0.3	2.0	3.0	0.08
18	11.4 ± 1.2	8.9 ± 0.7	4.2 ± 1.1	7.8 ± 1.9	0.7	0.9	1.9
19	12.4 ± 1.5	15.5 ± 1.5	16.8 ± 0.7	25.1 ± 0.3	2.0	1.6	1.5

[a]IC_{50} values are expressed as the compound concentration (nM) that inhibits the cell growth by 50%. Data are the average (±SD) of three experiments. [b]SI_A = IC_{50}(HEK-293)/IC_{50}(HT-29). [c]SI_B = IC_{50}(HEK-293)/IC_{50}(MCF-7). [d]SI_C = IC_{50}(HEK-293)/IC_{50}(A549).

The observed IC_{50} values are all in the low nanomolar range. In the case of the HT-29 cell line, all compounds show a better antiproliferative activity than colchicine itself. It is worth noting that derivative **17** exhibits in HT-29 and MCF-7 cell lines a very low IC_{50} value situated in the picomolar range, therefore two orders of magnitude lower than the natural product. As for the A549 cell line, most compounds exhibit IC_{50} values in the same range as the natural alkaloid. Interestingly, most compounds exhibit SI values greater than colchicine. The haloacetyl derivatives **1-4** show lower SI values than those having aroyl moieties, the most selective derivatives among the latter being **8** (2-MePh) and **15** (4-ClPh). Particularly worth mentioning is compound **17** (3-BrPh), which combines a picomolar anti-

proliferative activity with high SI values in the HT-29 and MCF-7 cell lines. These synthetic compounds therefore could offer the possibility of use in cancer therapy with lower dosages than colchicine, this resulting in less acute toxicity problems than in the case of the natural alkaloid.

Further biological studies have been carried out in order to establish whether the observed antiproliferative effect in cells is due to the interaction of these colchicine derivatives with tubulin. These studies are detailed hereafter.

2.3.2. Effects on tubulin assembly

With the aim of studying the effects of our derivatives on tubulin self-assembly, the critical concentration for compounds **1-19** was determined in glycerol-assembling buffer (GAB). The results are compared with those achieved in the presence of colchicine and also of podophyllotoxin, a further microtubule-destabilizing agent. A solution of 25 μM tubulin was incubated at 37ºC with 27.5 μM concentrations of colchicine, podophyllotoxin and compounds **1-19**. Table 2 summarizes the results achieved.

Table 2. Critical concentration (CrC) for the assembly of purified tubulin in GAB in the presence of colchicine, podophyllotoxin and the colchicine analogues **1-19**.[a]

Compound	**CrC** (μM)
Control	9± 2
Colchicine	24.5 ± 0.3
Podophyllotoxin	23.5 ± 0.7
1	24.6 ± 0.3
2	24.7 ± 0.2
3	24.6 ± 0.6
4	24.2 ± 0.3
5	22.9 ± 1.5
6	24.1 ± 0.4
7	23.9 ± 0.7
8	19.9 ± 1.5
9	23.4 ± 1.1
10	21.1 ± 1.5
11	14.0 ± 0.9
12	22.9 ± 1.3

13	24.1 ± 0.8
14	23.6 ± 0.5
15	24.9 ± 0.4
16	19.5 ± 0.6
17	23.5 ± 1.1
18	19.9 ± 1.4
19	20 ± 2

[a] Data are the average (±SD) of three experiments.

All colchicine derivatives inhibit microtubule formation with the exception of compound **11** (4-*n*-PentPh), which shows very little activity. Indeed, the concentration of tubulin required to produce assembly raises from 9 μM in the absence of the drugs (DMSO vehicle as control) to a maximum value of 24.9 μM in the presence of compound **15** (4-ClPh), comparable with that showed by colchicine (24.5 μM) and podophyllotoxin (23.5 μM). The critical concentration values of analogues **1**–**19** (except for **11**) therefore confirm that the observed antiproliferative effect in cells is due to their interaction with tubulin.

Figure 4 depicts the effects of the ligands on the kinetics of tubulin self-assembly. As can be observed, thirteen of the synthetic compounds showed a full inhibition of microtubule formation in the same way as colchicine (CLC in the figure). Derivatives **8** (2-MePh), **10** (4-MePh), **16** (2-BrPh) and **18** (4-BrPh) and **19** caused partial inhibition of microtubule formation and also a delay on the polymerization process.

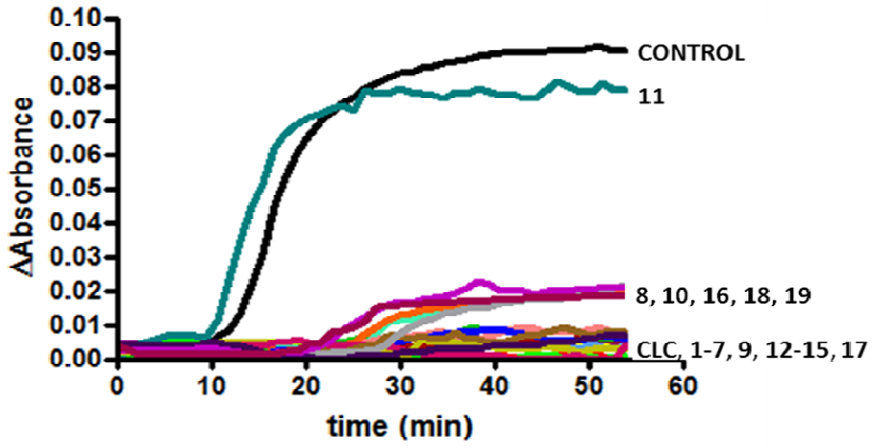

Figure 4. Effects of colchicine and compounds **1**-**19** on the kinetics of tubulin assembly. The lines in the figure show the turbidity time course of polymerization of tubulin alone (black) at 25 μM,

colchicine (red), **8** (green), **10** (orange), **16** (gray) and **18** (purple) and **19** (pink). All compounds were at 27.5 μM.

In order to quantify this delay of the nucleation and elongation process, we have calculated the It_{50} value, defined as the time needed to reach 50% of the polymerization equilibrium. The It_{50} values obtained for the control (DMSO) and compounds **8** (2-MePh), **10** (4-MePh), **16** (2-BrPh) and **18** (4-BrPh) and **19** are shown in Table 3.

Table 3. It_{50} of some compounds for tubulin self-assembly.[a]

Compound	**Control**	**8**	**10**	**16**	**18**	**19**
It_{50} (min)	16.5 ± 0.8	32.6 ± 0.3	28.8 ± 1.0	34.0 ± 0.5	27 ± 3	27±5

[a] Data are the average (±SD) of three experiments.

Compounds having a comparatively high value of critical concentration with respect to the control (lower absorbance in the stationary phase), as well as a higher It_{50} value with respect to the control (increased time required for nucleation and elongation) are considered as partial inhibitors of the polymerization of tubulin. This is the case of compounds **8**, **10**, **16**, **18** and **19**.

2.3.3. Effects on the cell cycle

Having established that our colchicine derivatives inhibit *in vitro* microtubule assembly, it was convenient to ascertain whether they also could inhibit microtubule polymerization inside cells causing cell cycle arrest, and also to characterize their effects on microtubules, mitoses and DNA content. First of all, we selected the most active compounds for a study of the effects on the morphology of A549 cells after 24 h treatment with different concentrations of our compounds. As a matter of fact, most of the A549 cells became rounded mitotic cells in the presence of colchicine, deacetylcolchicine **19** and compounds **1**-**4**, **6**-**10**, **13**-**15** and **16**-**18.** However, the cell morphology was not significantly affected after treatment with **5** ($CH_2C_6H_{11}$), **11** (4-*n*-PentPh) and **12** (4-*t*-BuPh), as compared with the control cells, with only some small, round and non-adherent cells being observed. For this reason, these three derivatives were discarded for cell cycle studies. The main results are summarized in Table 4.

Table 4. Cell cycle distribution for colchicine and selected compounds.[a]

Compound	**Conc. (nM)**	**Sub G0**	**G0/G1**	**S**	**G2/M**
Control		2 ± 1	73 ± 3	15 ± 6	11 ± 4
Colchicine	50	3 ± 1	27 ± 14	11 ± 2	59 ± 17

1	*7.5*	*2 ±1*	*25 ±6*	*15 ±9*	*60 ±13*
2	*15*	*2 ±1*	*22 ±7*	*20 ±3*	*55 ±9*
3	*15*	*3 ±1*	*25 ±3*	*19 ±3*	*53 ±4*
4	150	7 ± 3	17 ± 3	13 ± 2	62 ± 2
6	20	5 ± 1	19 ± 2	16 ± 2	60 ± 2
7	50	4 ± 3	29 ± 6	28 ± 10	40 ± 6
8	50	8 ± 2	24 ± 5	14 ± 2	47 ± 5
9	50	16 ± 6	29 ± 8	10 ± 1	45 ± 1
10	50	13 ± 5	44 ± 6	26 ± 2	16 ± 1
13	*15*	*3 ±1*	*11 ±1*	*26 ±10*	*55 ±1*
14	20	6 ± 1	24 ± 5	15 ± 1	57 ± 8
15	15	2 ± 1	27 ± 3	14 ± 4	48 ± 11
16	20	4 ± 3	27 ± 1	22 ± 4	47 ± 6
17	20	4 ± 3	29 ± 1	16 ± 3	51 ± 3
18	20	4 ± 3	25 ± 3	16 ± 1	56 ± 1
19	150	5 ± 1	47 ± 6	15 ± 3	33 ± 2

[a] Concentration in italics corresponds approximately to the IC_{50} value. Data are the average (±SD) of two experiments.

The observed results show that all compounds except **10** (4-MePh) and **19** (lacking any acyl group), are able to arrest the cell cycle at the G2/M phase. Some of these derivatives have been studied at different concentrations in order to see which are the most active compounds at the lowest concentration. In all cases, a sub-G1 peak, presumably of cells undergoing apoptosis, was observed. *Ortho*-, *meta*- and *para*-chloro and bromobenzoyl derivatives **13**-**18** cause interruption of the cell cycle at the G2/M phase when tested at approximately 20 nM. However, at 3 nM concentration, derivatives **13-18** accumulate cells in G2/M phase in a higher percentage than in the control. Fluoroacetyl and chloroacetyl derivatives **1** and **2**, respectively, arrest the cell cycle at the G2/M phase at their IC_{50} concentration. Interestingly, the bromoacetyl derivative **3** is able to block the cell cycle at the G2/M phase at half the value of its IC_{50}. Iodoacetyl derivative **4** is the less active one of these series of haloacetyl compounds.

2.3.4. Effect of selected derivatives on the expression of hTERT and c-MYC genes

In order to expand our research on colchicine derivatives with potential utility in cancer therapy, we proceeded to investigate the effect they exert on the expression of *c-Myc*, *hTERT* and *VEGF* genes as well as VEGF protein secretion on HT-29 cell line.

First of all, a preliminary study was carried out by conventional PCR to qualitatively determine which compounds were able to modify the expression of these three genes after 48 h of treatment in the HT-29 cell line (data not shown). This preliminary test let us select twelve derivatives and their minimal active concentration (see Figure 5) for a quantitative study of gene expression on the same cell line.

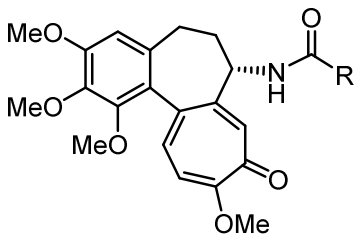

Colchicine R = Me (10 nM and 40 nM)

1	R = CH_2F	3 nM	**13**	R = 2-ClC_6H_4	1.5 nM
2	R = CH_2Cl	3 nM	**14**	R = 3-ClC_6H_4	1.5 nM
3	R = CH_2Br	10 nM	**15**	R = 4-ClC_6H_4	1.5 nM
4	R = CH_2I	10 nM	**16**	R = 2-BrC_6H_4	5 nM
9	R = 3-MeC_6H_4	2 nM	**17**	R = 3-BrC_6H_4	0.5 nM
12	R = 4-*t*BuPh	30 nM	**18**	R = 4-BrC_6H_4	9 nM

Figure 5. Selected compounds and concentrations for a quantitative gene expression test

As regards the ability of our compounds for the inhibition of the *c-Myc* gene expression, we found that colchicine was very active at a concentration of 40 nM but has no activity when tested at 10 nM (see Figure 6, panel A). Special attention must be paid on chloroaroyl derivatives **13**-**15** and *meta*-bromoaroyl compound **17**, because they were able to inhibit more than 60% of *c-MYC* gene expression at very low concentration (1.5 nM for all of them except for **17** that was 0.5 nM). Bromoacetyl derivative **3** was also more active than colchicine itself as it was able to inhibit to 35% of gene expression at a concentration 13 times lower than the natural product.

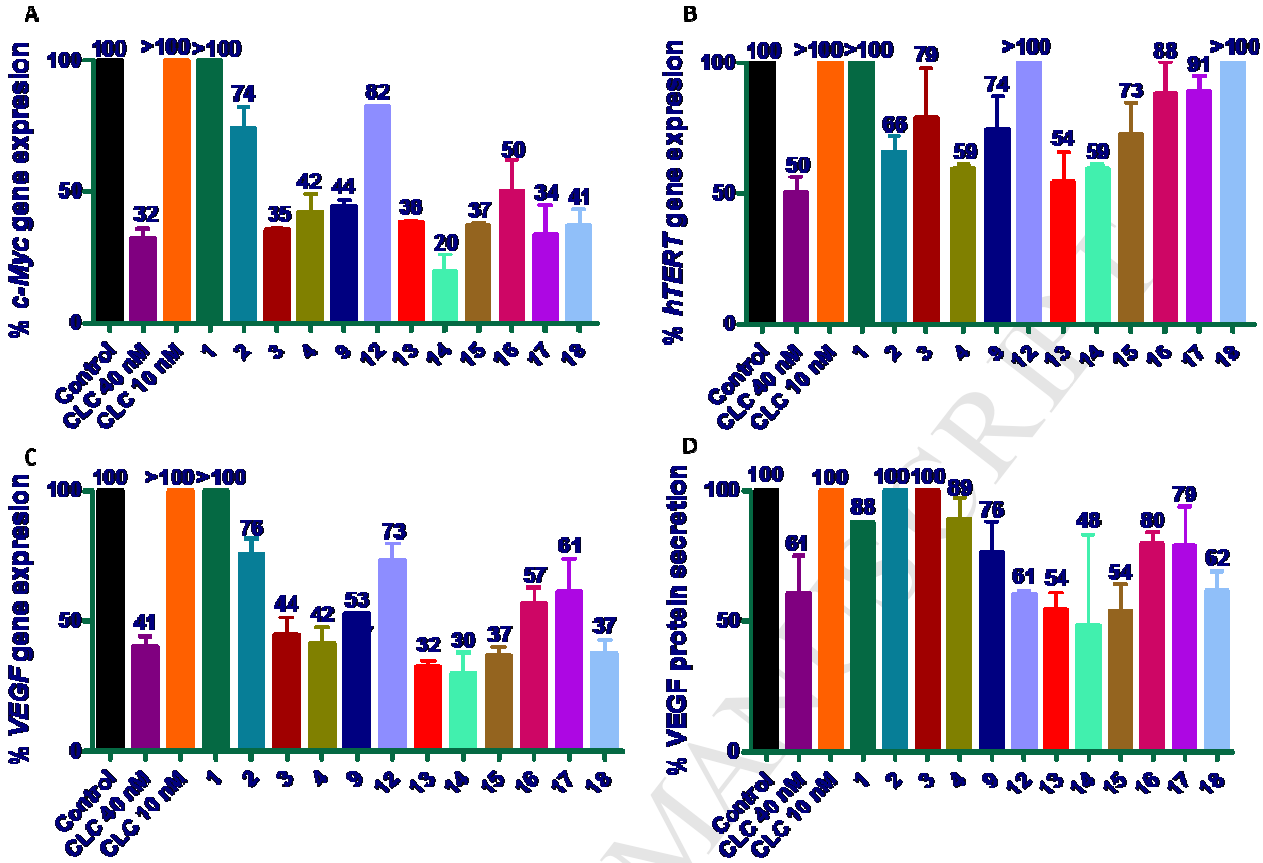

Figure 6. Panel A: Expression percentage of the *c-Myc* gene after 48 h of incubation with DMSO (control) and the selected compounds. **Panel B:** Expression percentage of the *hTERT* gene after 48 h of incubation with DMSO (control), and the selected compounds. **Panel C:** Expression percentage of the *VEGF* gene after 48 h of incubation with DMSO (control), and the selected compounds. **Panel D:** Expression percentage of the VEGF protein secreted after 48 h of incubation with DMSO (control), and the selected compounds. At least three measurements were performed in each case Gene expression was normalized using *β-ACTIN* as endogenous gene. Gene expression was normalized using β-*ACTIN* as endogenous gene. Percentages above 100% indicate that the corresponding compounds were less active than the control. Error bars indicate standard errors of the mean. The statistical significance was evaluated using one-sample *t*-tests (P <0.001).

As regards the ability of our compounds to inhibit *hTERT* gene expression, we found that colchicine was able to inhibit to half the expression of this gene at a concentration of 40 nM but had no activity when tested at 10 nM (see Figure 6, panel B). In this case, *o*- and *m*-chloroaroyl derivatives **13** and **14** were the most active ones as they caused more than 40% of *hTERT* gene inhibition at a concentration of 1.5 nM. The iodoacetyl derivative **4** was also fairly active as it was able to downregulate gene expression to 40% at a concentration of 3 nM.

As regards inhibition of *VEGF* gene expression, we found that colchicine was active at a concentration of 40 nM but had no activity when tested at 10 nM (see Figure 6, panel C). Again, chloroaroyl derivatives **13**-**15** showed the best activities as they were able to inhibit more than 70% of *VEGF* gene expression at a concentration of 1.5 nM. *p*-Bromoderivative **18** ahowed also a good activity at 9 nM while *o*-bromoderivative **17** was able to inhibit about 40% of *VEGF* gene expression at 0.5 nM. In this case, the bromo and iodoacetyl derivatives **3** and **4** were also more active than colchicine itself as they were able to inhibit more than 50% of gene expression at a concentration 13 times lower than the natural product.

In order to check how the downregulation of *VEGF* gene expression by our derivatives affected VEGF protein secretion in HT-29 cell line, we evaluated the amount of this protein in the culture medium after 48 h of treatment (see Figure 6, panel D).7 This evaluation was carried out by ELISA measurements (see experimental section). The chloroaroyl derivatives **13**-**15** showed the best activities as they were able to inhibit to the half the secretion of the VEGF protein at a concentration of 1.5 nM. *p*-*t*-Butyl and *p*-bromoaroylderivatives **12** and **18** showed also activity similar to that of the natural product but at lower concentrations (30 nM and 9 nM respectively). In this case, the haloacetyl derivatives **1**-**4** were less active.

3. Conclusions

Colchicine analogues in which the *N*-acetyl residue has been replaced by *N*-haloacetyl, *N*-cyclohexylacetyl, *N*-phenylacetyl and *N*-aroyl moieties have been synthetized and their antiproliferative activities towards the tumor cell lines HT-29, MCF-7 and A549 and the non-tumor cell line HEK-293 have been measured. All derivatives show IC_{50} values in the low nanomolar range, with compound **17** showing a picomolar anti-proliferative action, two orders of magnitude more cytotoxic than colchicine. As regards the Selectivity Index (SI) values, most of the synthetic derivatives exhibit SI values greater than colchicine. Outstanding cases were those of derivatives **8** (2-MePh) and **15** (4-ClPh), with high SI values in the three tumor cell lines assayed, and of compound **17** (3-BrPh) with high SI values in the HT-29 and MCF-7 cell lines. These compounds therefore could offer the possibility of use in cancer therapy with lower dosages than colchicine, this resulting in less acute toxicity problems than in the case of the natural alkaloid.

As regards the tubulin polymerization process, compound **11** (4-*n*-PentPh) is the only one that showed a low ability to prevent microtubule formation. O*rtho*- and *para*-methylbenzoyl derivatives (**8**

and **10**) and o*rtho*- and *para*-bromobenzoyl derivatives (**16** and **18**) may be considered as partial inhibitors of tubulin polymerization. The remaining derivatives behave like colchicine and can be considered full tubulin polymerization inhibitors, compound **15** (4-ClPh) being the most active. The critical concentration values of analogues **1**–**18** (except for **11**) confirm that the observed antiproliferative effect in cells is due to their interaction with tubulin.

It is worth mentioning that the tested derivatives cause extensive arrest of the cell cycle at the G2/M phase with concentrations and incubation times identical to those of colchicine at 50 nM. Fluoro and chloroacetyl derivatives **1** and **2**, respectively, arrest the cell cycle at the G2/M phase when assayed at their IC_{50} concentration. Interestingly, bromoacetyl derivative **3** is able to block the cell cycle at the G2/M phase at half the value of its IC_{50} concentration. *Ortho*-, *meta*- and *para*-chloro and bromobenzoyl derivatives **13**-**18** cause interruption of the cell cycle at the G2/M phase when tested at approximately 20 nM.

These colchicine derivatives derivatives are also fairly active downregulating the expression of *c-MYC*, *hTERT* and *VEGF* genes.

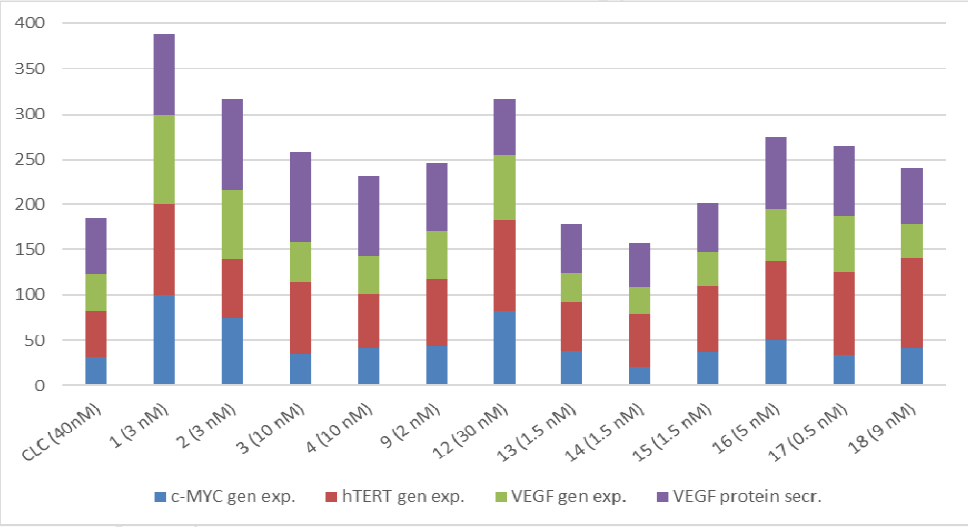

Figure 7. Percentage of the oncogene expressions and VEGF protein secretion in the presence of the selected derivatives.

The most active derivatives, along with colchicine, were those with a chloroaroyl unit **13**-**15**. These were able to downregulate the expression of *c-MYC*, *hTERT* and *VEGF* genes at 1.5 nM, a much lower concentration than the one needed to exert an anti-mitotic effect (see Table 4). The most active was m-chloroaroylderivative **14**, which reduced the expression of the *c-Myc*, *hTERT* and *VEGF* genes to 20%, 59% and 30%, respectively. In this sense, it is also worth mentioning that the *m*-

bromoaroylderivative **17** shows activity in downregulating the selected gene expressions at 0.5 nM, the lowest concentration observed in all these derivatives.

In summary, we have found that haloaroyl moiety is the responsible for the enhanced oncogene downregulation effect of these colchicine derivatives. We could conclude that the enhanced oncogene downregulation effect of compounds **13**-**15**, achieved at concentrations lower than their IC_{50} values, might broaden the therapeutic window of these compounds. Indeed, they could be good anti-cancer drug candidates because they decrease the expression of oncogenes involved in tumor aggressiveness at concentrations in which there is no antimitotic effect.

4. Experimental section

4.1. General procedures

NMR spectra were measured at 25°C. The signals of the deuterated solvent ($CDCl_3$) was taken as the reference. Multiplicity assignments of ^{13}C signals were made by means of the DEPT pulse sequence. Complete signal assignments in ^{1}H and ^{13}C NMR spectra were made with the aid of 2D homo- and heteronuclear pulse sequences (COSY, HSQC, HMBC). High resolution mass spectra were run by the electrospray mode (ESMS). IR data were measured with oily films on NaCl plates (oils) and are given only for relevant functional groups (C=O, NH). Optical rotations were measured at 25 °C. Experiments which required an inert atmosphere were carried out under dry N_2 in flame-dried glassware. THF was freshly distilled from sodium/benzophenone ketyl and transferred via syringe. Commercially available reagents were used as received. Where solutions were filtered through a Celite pad, the pad was additionally washed with the same solvent used, and the washings incorporated to the main organic layer.

*4.2. General procedure to prepare colchicine analogues **1**-**18**.*

Compound **19** (283 mg, 0.6 mmol) and the appropriate acid (1.2 mmol) were dissolved under N_2 in dry CH_2Cl_2 (60 mL) and treated with N,N'-dicyclohexylcarbodiimide (743 mg, 3.6 mmol) and 4-(N,N-dimethylamino)pyridine (147 mg, 1.2 mmol). The mixture was stirred for 3 h at room temperature and then filtered through Celite. The filtrate was evaporated under reduced pressure, and the residue was subjected to column chromatography on silica gel (EtOAc-acetone, 8:1) to afford the desired compound **1**-**18**. Yields ranked between 40 and 59%.

Yields: **1**, 58%; **2**, 56%; **3**, 51%; **4**, 43%; **5**, 54%; **6**, 52%; **7**, 45%; **8**, 59%; **9**, 54%; **10**, 54%; **11**, 53%; **12**, 46%; **13**, 51%; **14**, 55%; **15**, 53%; **16**, 49%; **17**, 51%; **18**, 58%.

4.2.1. **2-Fluoro-*N*-{(7*S*)-1,2,3,10-tetramethoxy-9-oxo-5,6,7,9-tetrahydrobenzo[a]heptalen-7-yl}acetamide:** yellowish solid, mp 103-105 °C, lit. [11a] mp 137-142 °C; $[\alpha]_D$ –140 (c, 1; $CHCl_3$); ^1H NMR ($CDCl_3$) δ 7.65 (1H, br d, *J* ~ 6.5 Hz, NH), 7.40 (1H, s), 7.25 (1H, d, *J* = 10.7 Hz), 6.80 (1H, d, *J* = 10.7 Hz), 6.50 (1H, s), 4.80-4.60 (3H, m), 3.95 (3H, s), 3.90 (3H, s), 3.87 (3H, s), 3.61 (3H, s), 2.51 (1H, dd, *J* = 13.7, 6.5 Hz), 2.39 (1H, apparent td, *J* = 13.2, 6.8 Hz), 2.26 (1H, m), 1.97 (1H, m); ^{13}C NMR ($CDCl_3$) δ 179.2, 167.1 (doublet with $^2J_{C-F}$ ~ 18.5 Hz), 163.9, 153.4, 151.1, 150.3, 141.6, 136.0, 133.9, 125.4 (C), 135.1, 130.6, 112.1, 107.3, 51.6 (CH), 80.0 (center point of doublet with $^1J_{C-F}$ ~ 185 Hz), 36.4, 29.7 (CH_2), 61.2, 61.1, 56.2, 56.0 (CH_3); IR ν_{max} 3270 br (NH), 1680 (C=O) cm^{-1}; HR ESMS *m/z* 440.1485 ($M+Na^+$). Calcd. for $C_{22}H_{24}FNNaO_6$, 440.1485.

4.2.2. **2-Chloro-*N*-{(7*S*)-1,2,3,10-tetramethoxy-9-oxo-5,6,7,9-tetrahydrobenzo[a]heptalen-7-yl} acetamide:** yellowish solid, mp 116-118 °C, lit. [11a] mp 204-206 °C; $[\alpha]_D$ –82 (c, 1; $CHCl_3$); ^1H NMR ($CDCl_3$) δ 8.15 (1H, br d, *J* ~ 6.5 Hz, NH), 7.45 (1H, s), 7.30 (1H, d, *J* = 10.7 Hz), 6.84 (1H, d, *J* = 10.7 Hz), 6.51 (1H, s), 4.63 (1H, apparent dt, *J* = 11.7, 6.5 Hz), 4.04-4.00 (2H, AB system, *J* = 14.5 Hz). 3.97 (3H, s), 3.91 (3H, s), 3.87 (3H, s), 3.62 (3H, s), 2.51 (1H, dd, *J* = 13.7, 6 Hz), 2.38 (1H, apparent td, *J* = 13.2, 6.7 Hz), 2.28 (1H, m), 1.94 (1H, m); ^{13}C NMR ($CDCl_3$) δ 179.3, 166.0, 164.1, 153.6, 151.2, 151.0, 141.7, 136.4, 134.0, 125.5 (C), 135.4, 130.6, 112.6, 107.4, 52.8 (CH), 42.5, 36.5, 29.8 (CH_2), 61.5, 61.4, 56.4, 56.1 (CH_3); IR ν_{max} 3270 br (NH), 1681 (C=O) cm^{-1}; HR ESMS *m/z* 456.1194 ($M+Na^+$). Calcd. for $C_{22}H_{24}{}^{35}ClNNaO_6$, 456.1190.

4.2.3. **2-Bromo-*N*-{(7*S*)-1,2,3,10-tetramethoxy-9-oxo-5,6,7,9-tetrahydrobenzo[a]heptalen-7-yl}acetamide:** brown-yellowish solid, mp 140-142 °C, lit. [11a] mp 203-206 °C; $[\alpha]_D$ –81 (c, 1; $CHCl_3$); ^1H NMR ($CDCl_3$) δ 8.40 (1H, br d, *J* ~ 6.5 Hz, NH), 7.52 (1H, s), 7.34 (1H, d, *J* = 10.7 Hz), 6.87 (1H, d, *J* = 10.7 Hz), 6.52 (1H, s), 4.63 (1H, apparent dt, *J* = 11.7, 6.5 Hz), 3.99 (3H, s), 3.93 (3H, s), 3.89 (3H, s), 3.95-3.85 (2H, m overlapped by the OMe signals), 3.64 (3H, s), 2.51 (1H, dd, *J* = 13.5, 6 Hz), 2.38 (1H, apparent td, *J* = 13, 6.5 Hz), 2.28 (1H, m), 1.90 (1H, m); ^{13}C NMR ($CDCl_3$) δ 179.3, 166.0, 164.0, 153.6, 151.4, 151.1, 141.7, 136.5, 134.0, 125.4 (C), 135.4, 130.4, 112.7, 107.4, 52.9 (CH), 36.4, 29.7, 28.7 (CH_2), 61.4, 61.3, 56.4, 56.1 (CH_3); IR ν_{max} 3260 br (NH), 1681 (C=O) cm^{-1}; HR ESMS *m/z* 500.0684 ($M+Na^+$). Calcd. for $C_{22}H_{24}{}^{79}BrNNaO_6$, 500.0685.

4.2.4. **2-Iodo-*N*-{(7*S*)-1,2,3,10-tetramethoxy-9-oxo-5,6,7,9-tetrahydrobenzo[a]heptalen-7-yl}acetamide:** brown-yellowish solid, mp 161-163 °C, lit. [11a] mp 195 °C; $[\alpha]_D$ –85 (c, 1; $CHCl_3$); ^1H NMR ($CDCl_3$) δ 8.70 (1H, br d, *J* ~ 7 Hz, NH), 7.64 (1H, s), 7.36 (1H, d, *J* = 10.7 Hz), 6.89 (1H, d, *J* = 10.7 Hz), 6.51 (1H, s), 4.63 (1H, apparent dt, *J* = 11.7, 6.5 Hz), 4.00 (3H, s), 3.93 (3H, s), 3.89 (3H, s), 3.82 (1H, d, *J* = 10.5 Hz), 3.77 (1H, d, *J* = 10.5 Hz), 3.65 (3H, s), 2.48 (1H, dd, *J* = 13, 6 Hz), 2.40-2.25 (2H, br m), 1.86 (1H, m); ^{13}C NMR ($CDCl_3$) δ 179.5, 167.6, 164.0, 153.5, 152.2, 151.1, 141.7, 136.8, 134.0, 125.4 (C), 135.5, 130.5, 112.9, 107.4, 52.9 (CH), 36.4, 29.8, −0.1 (CH_2), 61.5, 61.3, 56.4, 56.1 (CH_3); IR ν_{max} 3260 br (NH), 1675 (C=O) cm^{-1}; HR ESMS *m/z* 548.0537 ($M+Na^+$). Calcd. for $C_{22}H_{24}INNaO_6$, 548.0546.

4.2.5. **2-Cyclohexyl-*N*-{(7*S*)-1,2,3,10-tetramethoxy-9-oxo-5,6,7,9-tetrahydrobenzo[a]heptalen-7-yl}acetamide:** brown-yellowish solid, mp 226-229 °C; $[\alpha]_D$ −138 (c, 1; $CHCl_3$); ^1H NMR ($CDCl_3$) δ 7.49 (1H, s), 7.35 (1H, br d, *J* ~ 7 Hz, NH), 7.28 (1H, d, *J* = 10.7 Hz), 6.82 (1H, d, *J* = 10.7 Hz), 6.49 (1H, s), 4.64 (1H, apparent dt, *J* = 11.7, 6.5 Hz), 3.96 (3H, s), 3.91 (3H, s), 3.86 (3H, s), 3.63 (3H, s), 2.46 (1H, dd, *J* = 13, 6 Hz), 2.34 (1H, apparent td, *J* = 13.2, 6.8 Hz), 2.22 (1H, m), 2.05 (2H, apparent d, *J* = 7 Hz), 1.83 (1H, m), 1.75-1.50 (6H, br m), 1.20-1.00 (3H, br m), 0.87 (2H, m); ^{13}C NMR ($CDCl_3$) δ 179.3, 172.1, 163.9, 153.3, 152.0, 151.1, 141.5, 136.5, 134.1, 125.6 (C), 135.0, 130.7, 112.4, 107.3, 52.0, 34.9 (CH), 44.1, 36.7, 33.1, 33.0, 29.8, 26.1, 25.9, 25.8 (CH_2), 61.5, 61.2, 56.2, 56.0 (CH_3); IR ν_{max} 3280 br (NH), 1656 (C=O) cm^{-1}; HR ESMS *m/z* 504.2364 ($M+Na^+$). Calcd. for $C_{28}H_{35}NNaO_6$, 504.2362.

4.2.6. **2-Phenyl-*N*-{(7*S*)-1,2,3,10-tetramethoxy-9-oxo-5,6,7,9-tetrahydrobenzo[a]heptalen-7-yl}acetamide:** yellowish solid, mp 122-125 °C; $[\alpha]_D$ –99 (c, 1; $CHCl_3$); ^1H NMR ($CDCl_3$) δ 7.40-7.25 (7H, br m), 6.80 (1H, d, *J* = 10.7 Hz), 6.50 (1H, s), 5.90 (1H, br d, *J* ~ 7 Hz, NH), 4.62 (1H, apparent dt, *J* = 11.7, 6.5 Hz), 4.00 (3H, s), 3.94 (3H, s), 3.89 (3H, s), 3.66 (3H, s), 3.57 (2H, br s), 2.48 (1H, dd, *J* = 13.5, 6.5 Hz), 2.38 (1H, apparent td, *J* = 13.2, 6.5 Hz), 2.13 (1H, m), 1.65 (1H, apparent td, *J* = 12, 7 Hz); ^{13}C NMR ($CDCl_3$) δ 179.3, 170.6, 163.9, 153.4, 151.6, 151.1, 141.6, 136.5, 134.8, 134.1, 125.6 (C), 135.1, 130.6, 129.2 (x 2), 128.7 (x 2), 127.0, 112.4, 107.3, 52.2 (CH), 43.1, 36.6, 29.8 (CH_2), 61.5, 61.2, 56.2, 56.0 (CH_3); IR ν_{max} 3280 br (NH), 1653 (C=O) cm^{-1}; HR ESMS *m/z* 476.2083 ($M+H^+$). Calcd. for $C_{28}H_{30}NO_6$, 476.2073.

4.2.7. **_N_-{(7_S_)-1,2,3,10-tetramethoxy-9-oxo-5,6,7,9-tetrahydrobenzo[a]heptalen-7-yl}benzamide:** yellowish solid, mp 171-173 °C, lit. [11e] mp 150-152 °C; $[\alpha]_D$ –40 (c, 1.1; $CHCl_3$), lit. [15][1] $[\alpha]_D$ –107; ^{1}H NMR ($CDCl_3$) δ 7.90 (1H, br d, *J* ~ 7 Hz, NH), 7.77 (2H, d, *J* = 7.8 Hz), 7.63 (1H, s), 7.35-7.25 (2H, m), 7.19 (2H, t, *J* = 7.8 Hz), 6.85 (1H, d, *J* = 10.7 Hz), 6.53 (1H, s), 4.86 (1H, apparent dt, *J* = 11.5, 7 Hz), 3.97 (3H, s), 3.95 (3H, s), 3.89 (3H, s), 3.73 (3H, s), 2.49 (1H, dd, *J* = 13, 6.5 Hz), 2.43 (1H, apparent td, *J* = 13.5, 7 Hz), 2.40 (1H, m), 2.00 (1H, m); ^{13}C NMR ($CDCl_3$) δ 179.2, 166.9, 163.9, 153.4, 152.1, 151.1, 141.6, 136.5, 134.2, 133.3, 125.6 (C), 135.2, 131.3, 130.7, 128.1 (x 2), 127.0 (x 2), 112.4, 107.3, 52.7 (CH), 36.3, 29.9 (CH_2), 61.5, 61.2, 56.2, 56.0 (CH_3); IR ν_{max} 330 br (NH), 1654 (C=O) cm^{-1}; HR ESMS *m/z* 462.1915 ($M+H^+$). Calcd. for $C_{27}H_{28}NO_6$, 462.1916.

4.2.8. **2-Methyl-_N_-{(7_S_)-1,2,3,10-tetramethoxy-9-oxo-5,6,7,9-tetrahydrobenzo[a]heptalen-7-yl}benzamide:** yellowish solid, mp 202-205 °C; $[\alpha]_D$ –160 (c, 1.1; $CHCl_3$); ^{1}H NMR ($CDCl_3$) δ 7.46 (1H, s), 7.40 (1H, d, *J* = 7.5 Hz), 7.35-7.30 (2H, m), 7.20 (2H, m), 6.83 (1H, d, *J* = 10.7 Hz), 6.58 (1H, s), 6.20 (1H, br d, *J* ~ 7 Hz, NH), 4.85 (1H, apparent dt, *J* = 11.5, 7 Hz), 4.00 (3H, s), 3.97 (3H, s), 3.93 (3H, s), 3.72 (3H, s), 2.58 (1H, dd, *J* = 13, 6.5 Hz), 2.50 (1H, apparent td, *J* = 13.5, 7.2 Hz), 2.38 (3H, s), 2.35 (1H, m), 1.85 (1H, apparent td, *J* = 11.7, 6.8 Hz); ^{13}C NMR ($CDCl_3$) δ 179.2, 169.3, 163.9, 153.4, 151.2, 151.0, 141.6, 136.2, 136.0, 135.6, 134.1, 125.6 (C), 135.0, 130.8, 130.7, 129.7, 126.8, 125.5, 112.1, 107.3, 52.2 (CH), 36.9, 29.8 (CH_2), 61.4, 61.2, 56.1, 56.0, 19.7 (CH_3); IR ν_{max} 3260 br (NH), 1653 (C=O) cm^{-1}; HR ESMS *m/z* 476.2067 ($M+H^+$). Calcd. for $C_{28}H_{30}NO_6$, 476.2073.

4.2.9. **3-Methyl-_N_-{(7_S_)-1,2,3,10-tetramethoxy-9-oxo-5,6,7,9-tetrahydrobenzo[a]heptalen-7-yl}benzamide:** yellowish solid, mp 145-147 °C; $[\alpha]_D$ –48 (c, 1; $CHCl_3$); ^{1}H NMR ($CDCl_3$) δ 7.57 (1H, s), 7.54 (1H, br d, *J* ~ 7 Hz), 7.46 (1H, s), 7.33 (1H, d, *J* = 10.7 Hz), 7.30-7.25 (2H, m) 6.83 (1H, d, *J* = 10.7 Hz), 6.70 (1H, br d, *J* ~ 7 Hz, NH), 6.57 (1H, s), 4.86 (1H, apparent dt, *J* = 11.7, 7 Hz), 4.00 (3H, s), 3.97 (3H, s), 3.92 (3H, s), 3.73 (3H, s), 2.59 (1H, dd, *J* = 13, 6.5 Hz), 2.50 (1H, apparent td, *J* = 13, 7 Hz), 2.37 (3H, s), 2.40-2.35 (1H, m), 1.95 (1H, apparent td, *J* = 11.7, 6.8 Hz); ^{13}C NMR ($CDCl_3$) δ 179.2, 166.9, 163.9, 153.4, 152.1, 151.1, 141.6, 137.8, 136.6, 134.2, 133.2, 125.6 (C), 135.1, 132.0, 130.8, 128.0, 127.5, 124.1, 112.5, 107.3, 52.7 (CH), 36.4, 29.9 (CH_2), 61.5, 61.3, 56.2, 56.0, 20.9 (CH_3); IR ν_{max} 3290 br (NH), 1653 (C=O) cm^{-1}; HR ESMS *m/z* 476.2079 ($M+H^+$). Calcd. for $C_{28}H_{30}NO_6$, 476.2073.

4.2.10. **4-Methyl-*N*-{(7*S*)-1,2,3,10-tetramethoxy-9-oxo-5,6,7,9-tetrahydrobenzo[a]heptalen-7-yl}benzamide:** yellowish solid, mp 179-181 °C; $[\alpha]_D$ –28 (c, 1; $CHCl_3$); ^{1}H NMR ($CDCl_3$) δ 7.67 (2H, d, *J* = 7.8 Hz), 7.49 (1H, s), 7.33 (1H, d, *J* = 10.7 Hz), 7.16 (2H, d, *J* = 7.8 Hz) 6.90 (1H, br d, *J* ~ 7 Hz, NH), 6.83 (1H, d, *J* = 10.7 Hz), 6.56 (1H, s), 4.86 (1H, apparent dt, *J* = 11.7, 7 Hz), 3.99 (3H, s), 3.96 (3H, s), 3.91 (3H, s), 3.73 (3H, s), 2.57 (1H, dd, *J* = 13, 6.5 Hz), 2.48 (1H, apparent td, *J* = 13, 7 Hz), 2.40-2.30 (1H, m), 2.35 (3H, s), 1.95 (1H, apparent td, *J* = 11.7, 6.8 Hz); ^{13}C NMR ($CDCl_3$) δ 179.2, 166.8, 163.9, 153.4, 152.1, 151.2, 141.6 (x 2), 136.6, 134.2, 130.4, 125.6 (C), 135.1, 130.7, 128.8 (x 2), 127.0 (x 2), 112.4, 107.3, 52.7 (CH), 36.4, 29.9 (CH_2), 61.5, 61.3, 56.2, 56.0, 21.2 (CH_3); IR ν_{max} 3300 br (NH), 1652 (C=O) cm^{-1}; HR ESMS *m/z* 476.2070 ($M+H^+$). Calcd. for $C_{28}H_{30}NO_6$, 476.2073.

4.2.11. **4-(*n*-Pentyl)-*N*-{(7*S*)-1,2,3,10-tetramethoxy-9-oxo-5,6,7,9-tetrahydrobenzo[a]heptalen-7-yl}benzamide:** yellowish solid, mp 136-138 °C; $[\alpha]_D$ –20 (c, 0.96; $CHCl_3$); ^{1}H NMR ($CDCl_3$) δ 7.67 (2H, d, *J* = 7 Hz), 7.47 (1H, s), 7.33 (1H, d, *J* = 10.7 Hz), 7.18 (2H, d, *J* = 7 Hz), 6.82 (2H, m), 6.56 (1H, s), 4.86 (1H, apparent dt, *J* = 11.7, 7 Hz), 3.98 (3H, s), 3.96 (3H, s), 3.91 (3H, s), 3.73 (3H, s), 2.65-2.55 (3H, br m), 2.48 (1H, apparent td, *J* = 13, 7 Hz), 2.40-2.30 (1H, m), 1.94 (1H, apparent td, *J* = 11.5, 7 Hz), 1.65-1.55 (2H, m), 1.35-1.20 (4H, m), 0.89 (3H, t, *J* = 6.5 Hz); ^{13}C NMR ($CDCl_3$) δ 179.3, 166.9, 164.0, 153.4, 151.7, 151.2, 146.8, 141.7, 136.4, 134.2, 130.8, 125.7 (C), 135.1, 130.7, 128.3 (x 2), 127.0 (x 2), 112.4, 107.4, 52.6 (CH), 36.7, 35.7, 31.3, 30.7, 29.9, 22.4 (CH_2), 61.6, 61.3, 56.2, 56.0, 13.9 (CH_3); IR ν_{max} 3290 br (NH), 1653 (C=O) cm^{-1}; HR ESMS *m/z* 532.2705 ($M+H^+$). Calcd. for $C_{32}H_{38}NO_6$, 532.2699.

4.2.12. **4-(*tert*-Butyl)-*N*-{(7*S*)-1,2,3,10-tetramethoxy-9-oxo-5,6,7,9-tetrahydrobenzo[a]heptalen-7-yl}benzamide:** yellowish solid, mp 163-165 °C; $[\alpha]_D$ –28 (c, 1; $CHCl_3$); ^{1}H NMR ($CDCl_3$) δ 7.70 (2H, d, *J* = 7 Hz), 7.44 (1H, s), 7.43 (2H, d, *J* = 7 Hz), 7.33 (1H, d, *J* = 10.7 Hz), 6.82 (1H, d, *J* = 10.7 Hz), 6.60 (1H, br d, *J* ~ 7 Hz, NH), 6.57 (1H, s), 4.87 (1H, apparent dt, *J* = 11.7, 7 Hz), 3.99 (3H, s), 3.97 (3H, s), 3.92 (3H, s), 3.74 (3H, s), 2.57 (1H, dd, *J* = 13, 6.5 Hz), 2.50 (1H, apparent td, *J* = 13, 7 Hz), 2.40-2.30 (1H, m), 1.92 (1H, apparent td, *J* = 11.5, 7 Hz), 1.33 (9H, s); ^{13}C NMR ($CDCl_3$) δ 179.3, 166.9, 163.9, 154.8, 153.4, 151.8, 151.2, 141.6, 136.4, 134.2, 130.6, 125.7, 34.7 (C), 135.1, 130.7, 126.9 (x 2), 125.2 (x 2), 112.4, 107.4, 52.6 (CH), 36.6, 29.9 (CH_2), 61.6, 61.3, 56.2, 56.0, 31.0 (x 3) (CH_3); IR ν_{max} 3300 br (NH), 1652 (C=O) cm^{-1}; HR ESMS *m/z* 518.2549 ($M+H^+$). Calcd. for $C_{31}H_{36}NO_6$, 518.2543.

4.2.13. **2-Chloro-*N*-{(7*S*)-1,2,3,10-tetramethoxy-9-oxo-5,6,7,9-tetrahydrobenzo[a]heptalen-7-yl}benzamide:** yellowish solid, mp 153-155 °C; $[\alpha]_D$ −134 (c, 1; $CHCl_3$); ^{1}H NMR ($CDCl_3$) δ 7.64 (1H, d, *J* = 7.5 Hz), 7.48 (1H, s), 7.40-7.30 (4H, br m), 6.85-6.80 (2H, m), 6.57 (1H, s), 4.87 (1H, apparent dt, *J* = 11.5, 7 Hz), 3.99 (3H, s), 3.96 (3H, s), 3.92 (3H, s), 3.72 (3H, s), 2.58 (1H, dd, *J* = 13, 6.5 Hz), 2.49 (1H, apparent td, *J* = 13.2, 7 Hz), 2.40 (1H, m), 1.92 (1H, apparent td, *J* = 11.5, 6.5 Hz); ^{13}C NMR ($CDCl_3$) δ 179.2, 165.8, 163.9, 153.4, 151.1, 150.5, 141.6, 136.0, 134.4, 134.0, 130.5, 125.6 (C), 134.9, 131.1, 131.0, 130.0, 129.8, 126.8, 112.1, 107.3, 52.6 (CH), 36.8, 29.8 (CH_2), 61.4, 61.2, 56.1, 56.0 (CH_3); IR ν_{max} 3250 br (NH), 1666 (C=O) cm^{-1}; HR ESMS *m/z* 496.1523 ($M+H^+$). Calcd. for $C_{27}H_{27}{}^{35}ClNO_6$, 496.1527.

4.2.14. **3-Chloro-*N*-{(7*S*)-1,2,3,10-tetramethoxy-9-oxo-5,6,7,9-tetrahydrobenzo[a]heptalen-7-yl}benzamide:** yellowish solid, mp 105-107 °C; $[\alpha]_D$ −15 (c, 0.92; $CHCl_3$); ^{1}H NMR ($CDCl_3$) δ 7.85 (1H, br s, NH), 7.74 (1H, s), 7.62 (2H, m), 7.47 (1H, d, *J* = 10.7 Hz), 7.33 (1H, d, *J* = 7.8 Hz), 7.17 (1H, t, *J* = 7.8 Hz), 6.89 (1H, d, *J* = 10.7 Hz), 6.56 (1H, s), 4.87 (1H, apparent dt, *J* = 11.5, 7 Hz), 4.00 (3H, s), 3.96 (3H, s), 3.91 (3H, s), 3.73 (3H, s), 2.57 (1H, dd, *J* = 13, 6.5 Hz), 2.50-2.35 (2H, br m), 2.07 (1H, apparent td, *J* = 11.5, 6.5 Hz); ^{13}C NMR ($CDCl_3$) δ 179.2, 165.2, 164.1, 153.5, 152.4, 151.2, 141.6, 136.9, 134.8, 134.3, 130.5, 125.6 (C), 135.5, 131.3, 130.7, 129.5, 127.5, 125.0, 112.9, 107.4, 53.0 (CH), 36.2, 29.9 (CH_2), 61.6, 61.3, 56.4, 56.1 (CH_3); IR ν_{max} 3290 br (NH), 1662 (C=O) cm^{-1}; HR ESMS *m/z* 496.1527 ($M+H^+$). Calcd. for $C_{27}H_{27}{}^{35}ClNO_6$, 496.1527.

4.2.15. **4-Chloro-*N*-{(7*S*)-1,2,3,10-tetramethoxy-9-oxo-5,6,7,9-tetrahydrobenzo[a]heptalen-7-yl}benzamide:** yellowish solid, mp 122-124 °C; $[\alpha]_D$ +56.5 (c, 0.92; $CHCl_3$); ^{1}H NMR ($CDCl_3$) δ 7.73 (2H, d, *J* = 7.8 Hz), 7.62 (1H, s), 7.39 (1H, d, *J* = 10.7 Hz), 7.20-7.15 (3H, m), 6.90 (1H, d, *J* = 10.7 Hz), 6.55 (1H, s), 4.85 (1H, apparent dt, *J* = 11.5, 7 Hz), 4.00 (3H, s), 3.96 (3H, s), 3.91 (3H, s), 3.75 (3H, s), 2.60-2.55 (1H, m), 2.50-2.35 (2H, br m), 2.10-2.00 (1H, m); ^{13}C NMR ($CDCl_3$) δ 179.1, 165.7, 164.0, 153.5, 152.8, 151.2, 141.6, 137.4, 137.0, 134.2, 131.3, 125.5 (C), 135.6, 130.4, 128.5 (x 2), 128.3 (x 2), 112.9, 107.4, 53.2 (CH), 36.0, 30.0 (CH_2), 61.6, 61.3, 56.3, 56.1 (CH_3); IR ν_{max} 3290 br (NH), 1662 (C=O) cm^{-1}; HR ESMS *m/z* 496.1527 ($M+H^+$). Calcd. for $C_{27}H_{27}{}^{35}ClNO_6$, 496.1527.

4.2.16. **2-Bromo-*N*-{(7*S*)-1,2,3,10-tetramethoxy-9-oxo-5,6,7,9-tetrahydrobenzo[a]heptalen-7-yl}benzamide:** yellowish solid, mp 174-176 °C; $[\alpha]_D$ −152 (c, 1; $CHCl_3$); ^{1}H NMR ($CDCl_3$) δ 7.59 (1H, d, *J* = 7.8 Hz), 7.55 (1H, d, *J* = 7.8 Hz), 7.50 (1H, s), 7.40-7.30 (3H, br m), 6.82 (1H, d, *J* = 10.8 Hz),

6.57 (1H, s), 6.50 (1H, br d, $J \sim 7$ Hz, NH), 4.88 (1H, apparent dt, J = 11.3, 7 Hz), 4.00 (3H, s), 3.97 (3H, s), 3.93 (3H, s), 3.72 (3H, s), 2.58 (1H, dd, J = 13, 6.5 Hz), 2.50 (1H, apparent td, J = 13.2, 6.5 Hz), 2.44 (1H, m), 1.90 (1H, apparent td, J = 11.5, 6.5 Hz); ^{13}C NMR ($CDCl_3$) δ 179.2, 166.8, 163.9, 153.4, 151.1, 150.5, 141.6, 137.1, 136.1, 134.0, 125.6, 119.1 (C), 135.0, 133.0, 131.2, 131.1, 129.6, 127.4, 112.1, 107.4, 52.6 (CH), 36.9, 29.8 (CH_2), 61.4, 61.2, 56.1, 56.0 (CH_3); IR ν_{max} 3250 br (NH), 1665 (C=O) cm^{-1}; HR ESMS *m/z* 540.1019 (M+H$^+$). Calcd. for $C_{27}H_{27}{}^{79}BrNO_6$, 540.1022.

4.2.17. **3-Bromo-*N*-{(7*S*)-1,2,3,10-tetramethoxy-9-oxo-5,6,7,9-tetrahydrobenzo[a]heptalen-7-yl}benzamide:** yellowish solid, mp 137-139 °C; $[\alpha]_D$ –11 (c, 0.96; $CHCl_3$); ^{1}H NMR ($CDCl_3$) δ 8.50 (1H, br d, $J \sim 7$ Hz, NH), 7.90 (1H, br s), 7.68 (1H, s), 7.64 (1H, d, J = 7.8 Hz), 7.40 (1H, br d, $J \sim 8$ Hz), 7.38 (1H, d, J = 10.7 Hz), 6.99 (1H, t, J = 8 Hz), 6.90 (1H, d, J = 10.7 Hz), 6.52 (1H, s), 4.85 (1H, apparent dt, J = 11.5, 7 Hz), 3.99 (3H, s), 3.95 (3H, s), 3.89 (3H, s), 3.72 (3H, s), 2.49 (1H, dd, J = 13, 6 Hz), 2.45-2.30 (2H, br m), 2.13 (1H, m); ^{13}C NMR ($CDCl_3$) δ 179.2, 165.2, 164.1, 153.5, 152.4, 151.2, 141.6, 136.9, 134.8, 134.3, 130.5, 125.6 (C), 135.5, 131.3, 130.7, 129.5, 127.5, 125.0, 112.9, 107.4, 53.0 (CH), 36.2, 29.9 (CH_2), 61.6, 61.3, 56.4, 56.1 (CH_3); IR ν_{max} 3290 br (NH), 1654 (C=O) cm^{-1}; HR ESMS *m/z* 540.1025 (M+H$^+$). Calcd. for $C_{27}H_{27}{}^{79}BrNO_6$, 540.1022.

4.2.18. **4-Bromo-*N*-{(7*S*)-1,2,3,10-tetramethoxy-9-oxo-5,6,7,9-tetrahydrobenzo[a]heptalen-7-yl}benzamide:** yellowish solid, mp 154-156 °C; $[\alpha]_D$ +61.6 (c, 0.92; $CHCl_3$); ^{1}H NMR ($CDCl_3$) δ 7.80 (1H, br s, NH), 7.66 (2H, d, J = 8 Hz), 7.57 (1H, s), 7.40-7.35 (3H, m), 6.88 (1H, d, J = 10.8 Hz), 6.55 (1H, s), 4.84 (1H, apparent dt, J = 11.5, 7 Hz), 4.01 (3H, s), 3.97 (3H, s), 3.92 (3H, s), 3.74 (3H, s), 2.57 (1H, dd, J = 13, 6.5 Hz), 2.50-2.35 (2H, br m), 2.05-2.00 (1H, m); ^{13}C NMR ($CDCl_3$) δ 179.0, 165.7, 164.0, 153.5, 152.8, 151.1, 141.6, 137.0, 134.2, 131.7, 126.0, 125.5 (C), 135.6, 131.2 (x 2), 130.3, 128.7 (x 2), 113.0, 107.3, 53.2 (CH), 35.8, 29.9 (CH_2), 61.6, 61.2, 56.3, 56.0 (CH_3); IR ν_{max} 3290 br (NH), 1654 (C=O) cm^{-1}; HR ESMS *m/z* 540.1022 (M+H$^+$). Calcd. for $C_{27}H_{27}{}^{79}BrNO_6$, 540.1022.

4.3. Cell culture studies

Cell culture media were purchased from Gibco (Grand Island, NY). Fetal bovine serum (FBS) was a product of Harlan-Seralab (Belton, U.K.). Supplements and other chemicals not listed in this section were obtained from Sigma Chemical Co. (St. Louis, MO). Plastics for cell culture were supplied by

Thermo Scientific BioLite. All tested compounds were dissolved in DMSO at a concentration of 10 mM and stored at −20°C until use.

HT-29, MCF-7, A-549 and HEK-293 cell lines were maintained in Dulbecco's modified Eagle's medium (DMEM) containing glucose (1g/L), glutamine (2 mM), penicillin (50 IU/mL), streptomycin (50 μg/mL), and amphotericin B (1.25 μg/mL), supplemented with 10% FBS.

4.4. MTT assays

In order to study the antiproliferative capacity of our derivatives, we used MTT assay on HT-29, MCF-7, A-549 or HEK-293. 5,000 cells/well were placed in 96-well microtiter plate in a total volume of 100 μL of growth media. After 24 h, they were incubated with serial dilutions of the tested compounds. The 3-(4,5-dimethylthiazol-2-yl)-2,5-diphenyltetrazolium bromide (MTT; Sigma Chemical Co.) dye reduction assay in 96-well microplates was used, as previously described [26]. After 2 days of incubation (37 °C, 5% CO_2 in a humid atmosphere), 10 μL of MTT (5 mg/mL in phosphate-buffered saline, PBS) was added to each well, and the plate was incubated for a further 3 h (37 °C). The supernatant was discarded and replaced by 100 μL of DMSO to dissolve formazan crystals. The absorbance was then read at 540 nm by spectrophotometry. For all concentrations of compound, cell viability was expressed as the percentage of the ratio between the mean absorbance of treated cells and the mean absorbance of untreated cells. Three independent experiments were performed, and the IC_{50} values (i.e., concentration half inhibiting cell proliferation) were graphically determined.

4.5. Tubulin self-assembly measurements

Purified tubulin was used for these measurements. Tubulin polymerization was carried out in a 96 well plate. In each well 50 μL of a solution of 25 μM of tubulin in GAB buffer was added to 50 μL of 27.5 μM solution of the corresponding compounds in GAB buffer (20 mM sodium phosphate, 10 mM $MgCl_2$, 1 mM EGTA, 30% glycerol) and 0.1 mM GTP at pH = 6.5. Then, the plate was incubated at 37 ºC in Multiskan (R) and absorbance at 340 nM was registered every 30 seconds during 2 hours.

4.6. Cell cycle studies

Progression of the cell cycle was analysed by DNA determination by means of flow cytometry with propidium iodide. A549 cells were fixed, treated with RNase and stained with propidium iodide following instructions of BD CycletestTM DNA Kit. Analysis was performed with a BD AccuriTM C6 flow cytometer.

4.7. RT-qPCR Assay

HT-29 cells at 70–80% confluence were collected and 1.5 x 105 cells were placed in a six well plate in 1.5 mL of medium. After 24h, cells were incubated with the corresponding compounds for 48 h. Cells were collected and the total cellular RNA from HT-29 cells was isolated using Ambion RNA extraction Kit according to the manufacturer's instructions. The cDNA was synthesized by MMLV-RT with 1–21 μg of extracted RNA and oligo(dT)15 according to the manufacturer's instructions. Genes were amplified by use of a thermal cycler and StepOnePlus ™ Taqman ® probes. TaqMan ® Gene Expression Master Mix Fast containing the appropriate buffer for the amplification conditions, dNTPs, thermostable DNA polymerase enzyme and a passive reference probe was used. To amplify each of the genes the predesigned primers were used and sold by Life Technologies TaqMan ® Gene Expression Assays, Hs99999903-m1 (β-actin), Hs00972646-m1 (hTERT), Hs00153408-m1 (c-MYC) and Hs00900055-m1 (VEGF-A).

4.8. ELISA analysis

HT-29 cells at 70–80% confluence were collected and 1.5 x 10^5 cells were placed in a six well plate in 1.5 mL of medium. After 24h, cells were incubated with the corresponding compounds for 48 h. Culture supernatants were collected and VEGF secreted by HT-29 cells was determined using Invitrogen Human Vascular Endothelial Growth Factor ELISA Kit according to the manufacturer's instructions.

4.9. Molecular docking studies

Molecular docking was performed using Autodock 4.2 [9]. The crystal structure of αβ tubulin (PDB ID 1SA0) was used as a template. Nevertheless, the C and D subunits, stathmin, water molecules and bound ligands were previously removed from the protein structure in order to perform docking simulation. The GaussView 5.0 program [13] was used to build the structures of the colchicine derivatives **1**-**4** and **16**-**18**. Local docking was made in such a way that the grid box covered the entire αβ-tubulin interface. The grid map was used with 126 points equally in each x, y and z direction and with grid spacing 0.247 Å. The cluster was compared on the basis of the free energy of binding. The Lamarckian genetic algorithm (LGA) was employed with the default parameters; g_eval was set to 2500000 (medium) and 100 LGA runs were conducted. Molecular graphics were done with the program Visual Molecular Dynamics (VMD) [14]. Discovery Studio Visualizer program [15] has been used to show the interaction in 2-D between the compounds and the tubulin.

Acknowledgments

This research has been funded by the Ministerio de Economía y Competitividad (project CTQ2014-52949-P), by the Universitat Jaume I (project PI-1B2015-75) and by the Conselleria d'Educaciò, Investigaciò, Cultura i Sport de la Generalitat Valenciana (project PROMETEO 2013/027). A. M.-M. thanks the Conselleria d'Educaciò, Investigaciò, Cultura i Esport de la Generalitat Valenciana for a Ph. D. grant. The authors are also grateful to the SCIC of the Universitat Jaume I for providing NMR and mass spectrometry facilities.

Supplementary Information

Additional NMR data of all new synthetic compounds are provided in the Supplementary Information.

References

[1] P. Richette, T. Bardin, Colchicine for the treatment of gout. *Expert Opin. Pharmacother.* **2010**, *11*, 2933−2938. (b) N. Ozkaya, F. Yalçinkaya, Colchicine treatment in children with familial Mediterranean fever. *Clin Rheumatol.* **2003**, *22*, 314-317. (c) M. Imazio, A. Brucato, R. Cemin, S. Ferrua, et al., A Randomized Trial of Colchicine for Acute Pericarditis *N. Engl. J. Med.* **2013**, *369*, 1522-1528. (d) S. Yurdaku, C. Mat, Y. Tüzün, Y. Ozyazgan, V. Hamuryudan, O. Uysal, M. Senocak, H. Yazici, A double-blind trial of colchicine in Behçet's syndrome. *Arthritis Rheum.* **2001**, *44*, 2686-2692. (e) Roubille, F.; Kritikou, E.; Busseuil, D.; Barrere-Lemaire, S.; Tardif, J, C. Colchicine: an old wine in a new bottle? *Antiinflamm. Antiallergy Agents Med. Chem.* **2013**, *12*, 14-23. (f) D. C. Tong, A. M. Wilson, J. Layland, Colchicine in cardiovascular disease: an ancient drug with modern tricks. *Heart* **2016**, *102*, 995-1002.

[2] R.C. Weisenberg, G.G. Borisy, E.W. Taylor, The colchicine binding protein of mammalian brain and its relation to microtubules. *Biochemistry*, **1968**, *7*, 4466-4479.

[3] E. Ben-Chetrit, S. Bergmann, R. Sood, Mechanism of the anti-inflammatory effect of colchicine in rheumatic diseases: a possible new outlook through microarray analysis, *Rheumatology* **2006**, *45*, 274-282.

[4] S. Deftereos, G. Giannopoulos, N. Papoutsidakis, V. Panagopoulou, C. Kossyvakis, K. Raisakis, M.W. Cleman, C. Stefanadis, Colchicine and the heart: Pushing the envelope. *J. Am. Coll. Cardiol.* **2013**; *62*, 1817–1825.

[5] Y. Lu, J. Chen, M. Xiao, W. Li, D. D. Miller, An overview of tubulin inhibitors that interact with the colchicine binding Site. *Pharm Res.* **2012**, *29*, 2943-2971.

[6] C. Vilanova, S. Díaz-Oltra, J. Murga, E. Falomir, M. Carda, J. Alberto Marco, Inhibitory effect of pironetin/colchicine hybrids on the expression of the *VEGF*, *hTERT* and c-*MYC* genes, *Bioorganic and Med. Chem. Lett.* **2015**, *25*, 3194-3198.

[7] B.H.A. von Rahden, H. J. Stein, F. P. Oppermann, M. Sarbia, c-*MYC* Amplification is frequent in Esophageal Adenocarcinoma and Correlated with upregulation of *VEGF-A* expression, *Neoplasia* **2006**, *8*, 702-707

[8] S. Pelengaris, M. Khan, The c-Myc oncoprotein as a treatment target in cancer and other disorders of cell growth. *Expert Opin. Ther. Targets*, **2003**, *7*, 623-642.

[9] G. M. Morris, R. Huey, W. Lindstrom, M. F. Sanner, R. K. Belew, D. S. Goodsell, A. J. Olson, AutoDock4 and AutoDockTools4: Automated Docking with Selective Receptor Flexibility, *J. Comput Chem.* **2009**, *30*, 2785-2791.

[10] R. B. Ravelli, B. Gigant, P. A. Curmi, I. Jourdain, S. Lachkar, A. Sobel, et al., Insight into tubulin regulation from a complex with colchicine and a stathmin-like domain. *Nature* **2004**, 428, 198-202.

[11] J. D. Bagnato, A. L. Eilers, R. A. Horton, C. B Grissom, Synthesis and characterization of a cobalamin-colchicine conjugate as a novel tumor-targeted cytotoxin. *J. Org. Chem.* **2004**, *69*, 8987-8996.

[12] Compounds **1**-**4** have been previously described: (a) H. Lettré, K. H. Dönges, K. Barthold, T. J. Fitzgerald, Synthese neuerer Colchicin-Derivative mit hoher antimitotischer Wirksamkeit. *Liebigs Ann. Chem.* **1972**, *758*, 185-189. (b) F. R. Quinn, J. A. Beisler, Quantitative structure-activity relationships of colchicines against P388 leukemia in mice. *J. Med. Chem.* **1981**, *24*, 251-256. (c) F. R. Quinn, Z. Neiman, J. A. Beisler, Toxicity and quantitative structure-activity relationships of colchicines. *J. Med. Chem.* **1981**, *24*, 636–639. Compound **6** has been mentioned in: (d) D. J. Han, S. E. Yoo, J. Suh, . Patent: US2013/11417 A1, 2013. Compound **7** was first mentioned in: (e) F. Santavy, *Chemicke Listy* **1952**, *46*, 280-289. (f) Ref 9b and 9c. See also: (g) A. Brossi, P. N. Sharma, L. Atwell, A. E. Jacobson, et al., Biological effects of modified colchicines. 2. Evaluation of catecholic colchicines, colchifolines, colchicide, and novel N-acyl- and N-aroyldeacetylcolchicines. *J. Med. Chem.* **1983**, *26*, 1365–1369.

[13] R. Dennington, T. Keith, J. Millam, GaussView, Version 5, Semichem Inc., Shawnee Mission, KS, 2009.

[14] W. Humphrey, A. Dalke, K. Schulten, VMD: Visual Molecular Dynamics, *J. Molec. Graphics Model.* **1996**, *14*, 33-38.

[15] Dassault Systèmes BIOVIA, Discovery Studio Visualizer, v16.1.0.15350, San Diego: Dassault Systèmes, 2015.

List of captions

Figure 1. Structure of the colchicine analogues investigated in this study.

Figure 2. Panel A corresponds to the superimposition of the structures of **1** (black), **2** (orange), **3** (red) and **4** (purple) on the co-crystallized DAMA-colchicine (blue) at the colchicine binding site. Panel B corresponds to the structure of fluoroacetyl derivative **1** at the colchicine binding site. The α- and β-tubulin subunits are coloured in yellow and green, respectively.

Figure 3. Panel A corresponds to the superimposition of the structures of **16** (black), **17** (red) and **18** (purple) on the co-crystallized DAMA-colchicine (blue) at the colchicine binding site. Panel B, C and D correspond, respectively, to the structures of **16**, **17** and **18** at the colchicine binding site. The α- and β-tubulin subunits are coloured in yellow and green, respectively.

Scheme 1. Synthesis of colchicine derivatives **1-18**.

Table 1. IC_{50} values (nM) of synthetic compounds **1-19** in cancer cell lines HT-29, MCF-7 and A549, and one non-cancer cell line HEK-293.[a]

Table 2. Critical concentration (CrC) for the assembly of purified tubulin in GAB in the presence of colchicine, podophyllotoxin and the colchicine analogues **1-19**.[a]

Figure 4. Effects of colchicine and compounds **1-19** on the kinetics of tubulin assembly. The lines in the figure show the turbidity time course of polymerization of tubulin alone (black) at 25 µM, colchicine (red), **8** (green), **10** (orange), **16** (gray) and **18** (purple) and **19** (pink). All compounds were at 27.5 µM.

Table 3. It_{50} of some compounds for tubulin self-assembly.[a]

Table 4. Inhibitory Effects on Microtubule Assembly at 37ºC and 15 µM of tubulin.[a]

Figure 5. Selected compounds and concentrations for a quantitative gene expression test

Figure 6. Panel A: Expression percentage of the *c-Myc* gene after 48 h of incubation with DMSO (control) and selected compounds. **Panel B:** Expression percentage of the *hTERT* gene after 48 h of incubation with DMSO (control), and selected compounds. **Panel C:** Expression percentage of the *VEGF* gene after 48 h of incubation with DMSO (control), and selected compounds. **Panel D:** Expression percentage of the VEGF protein secreted after 48 h of incubation with DMSO (control), and selected compounds. At least three measurements were performed in each case Gene expression was normalized using *β-ACTIN* as endogenous gene. Gene expression was normalized using β-*ACTIN* as endogenous gene. Percentages above 100% indicate that the corresponding compounds were less active than the control. Error bars indicate standard errors of the mean. The statistical significance was evaluated using one-sample *t*-tests (P <0.001).

Figure 7. Percentage of the oncogene expressions and VEGF protein secretion in the presence of selected derivatives.

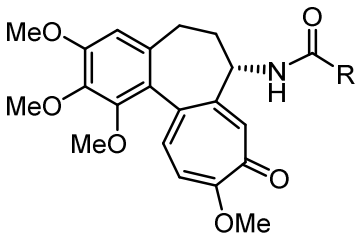

Colchicine R = Me

1 R = CH_2F
2 R = CH_2Cl
3 R = CH_2Br
4 R = CH_2I
5 R = 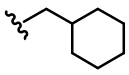
6 R = 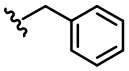

7 R = C_6H_5
8 R = 2-MeC_6H_4
9 R = 3-MeC_6H_4
10 R = 4-MeC_6H_4
11 R = 4-nC_5H_{11}Ph
12 R = 4-tBuPh

13 R = 2-ClC_6H_4
14 R = 3-ClC_6H_4
15 R = 4-ClC_6H_4
16 R = 2-BrC_6H_4
17 R = 3-BrC_6H_4
18 R = 4-BrC_6H_4

Figure 1.

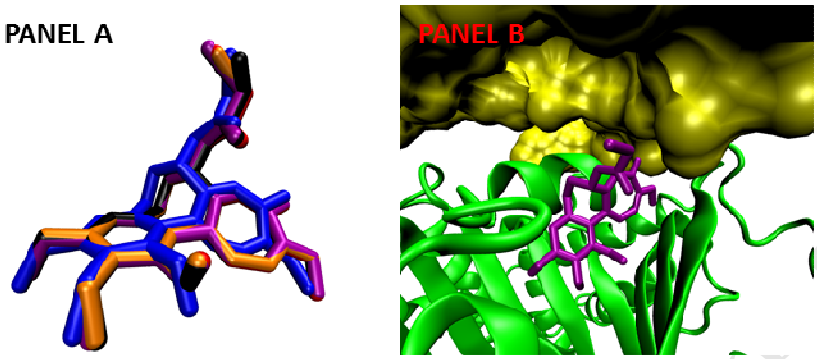

Figure 2

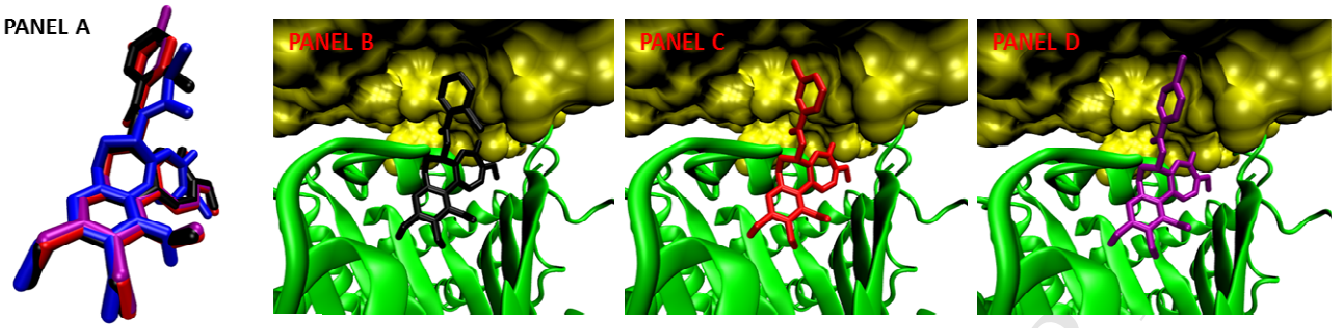

Figure 3

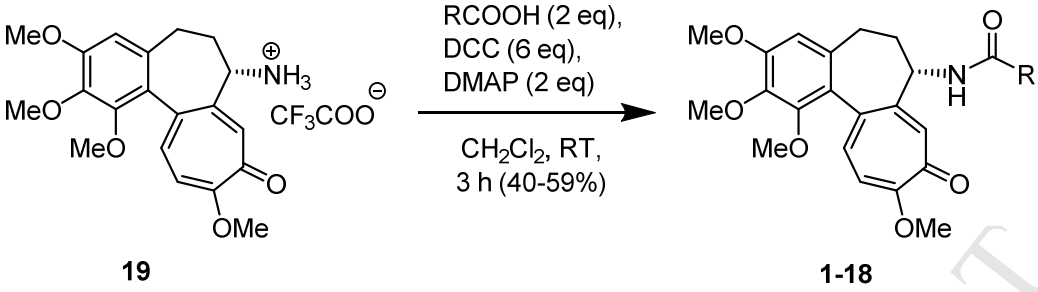

19 **1-18**

Scheme 1.

Table 1.

Compound	HT-29	MCF-7	A549	HEK-293	SI_A[b]	SI_B[c]	SI_C[d]
Colchicine	50 ± 3	12 ± 7	12.2 ± 0.7	5 ± 1	0.1	0.4	0.4
1	4.7 ± 1.3	7.3 ± 1.2	7.83 ± 0.15	7.1 ± 0.5	1.5	1.0	0.9
2	4.6 ± 0.4	29 ± 1	12.3 ± 2.1	4.56 ± 0.08	1.0	0.2	0.4
3	13.7 ± 0.2	16.4 ± 0.3	26 ± 5	14.36 ± 1.06	1.0	0.9	0.6
4	10 ± 1	4.1 ± 0.8	31 ± 3	19 ± 1	1.9	4.6	0.6
5	8.7 ± 0.5	9 ± 2	19.4 ± 3.1	10.5 ± 0.9	1.2	1.2	0.5
6	2.84 ± 0.04	2.6 ± 0.9	2.8 ± 0.9	3.9 ± 0.7	1.4	1.5	1.4
7	8.1 ± 0.9	5 ± 2	10 ± 3	13 ± 5	1.6	2.6	1.3
8	5.7 ± 0.5	2.02 ± 0.04	2.0 ± 0.6	9.0 ± 1.2	1.6	4.5	4.5
9	2.23 ± 0.23	5.6 ± 1.5	8.7 ± 1.3	3.1 ± 0.9	1.4	0.6	0.4
10	9.0 ± 2.2	31 ± 8	8.8 ± 1.2	16.1 ± 0.6	1.8	0.5	1.8
11	4.2 ± 1.2	5.8 ± 1.8	1.27 ± 0.4	1.6 ± 0.4	0.4	0.3	1.3
12	32.7 ± 2.1	24 ± 4	36 ± 6	58 ± 11	1.8	2.4	1.6
13	2.3 ± 0.4	4.5 ± 0.6	13 ± 3	5.93 ± 0.06	2.6	1.3	0.5
14	1.8 ± 0.3	3.4 ± 0.6	3.1 ± 1.1	3.0 ± 0.3	1.7	0.9	1.0
15	1.80 ± 0.15	6.7 ± 0.4	6.6 ± 1.0	10.1 ± 2.4	5.6	1.5	1.5
16	5.8 ± 0.3	7.6 ± 1.9	13 ± 3	8.5 ± 2.8	1.5	1.1	0.7
17	0.56 ± 0.04	0.363 ± 0.013	14 ± 4	1.1 ± 0.3	2.0	3.0	0.08
18	11.4 ± 1.2	8.9 ± 0.7	4.2 ± 1.1	7.8 ± 1.9	0.7	0.9	1.9
19	12.4 ± 1.5	15.5 ± 1.5	16.8 ± 0.7	25.1 ± 0.3	2.0	1.6	1.5

[a]IC_{50} values are expressed as the compound concentration (nM) that inhibits the cell growth by 50%. Data are the average (±SD) of three experiments. [b]SI_A = IC_{50}(HEK-293)/IC_{50}(HT-29). [c]SI_B = IC_{50}(HEK-293)/IC_{50}(MCF-7). [d]SI_C = IC_{50}(HEK-293)/IC_{50}(A549).

Table 2.

Compound	**CrC** (μM)
Control	9± 2
Colchicine	24.5 ± 0.3
Podophyllotoxin	23.5 ± 0.7
1	24.6 ± 0.3
2	24.7 ± 0.2
3	24.6 ± 0.6
4	24.2 ± 0.3
5	22.9 ± 1.5
6	24.1 ± 0.4
7	23.9 ± 0.7
8	19.9 ± 1.5
9	23.4 ± 1.1
10	21.1 ± 1.5
11	14.0 ± 0.9
12	22.9 ± 1.3
13	24.2 ± 0.8
14	23.6 ± 0.5
15	24.9 ± 0.4
16	19.5 ± 0.6
17	23.5 ± 1.1
18	19.9 ± 1.4
19	20 ± 2

[a] Data are the average (±SD) of three experiments.

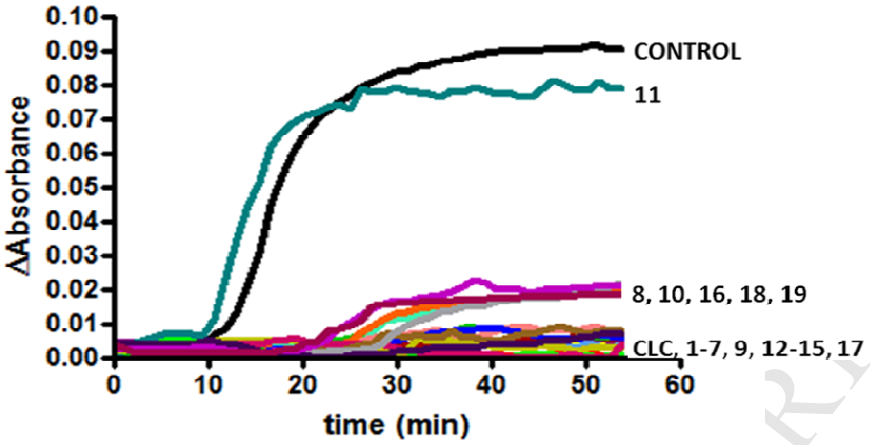

Figure 4.

Table 3.

Compound	Control	8	10	16	18	19
It_{50} (min)	16.5 ± 0.8	32.6 ± 0.3	28.8 ± 1.0	34.0 ± 0.5	27 ± 3	27±5

[a] Data are the average (±SD) of three experiments.

Table 4.

Compound	Conc. (nM)	Sub G0	G0/G1	S	G2/M
Control		2 ± 1	73 ± 3	15 ± 6	11 ± 4
Colchicine	50	3 ± 1	27 ± 14	11 ± 2	59 ± 17
1	*7.5*	*2 ±1*	*25 ±6*	*15 ±9*	*60 ±13*
2	*15*	*2 ±1*	*22 ±7*	*20 ±3*	*55 ±9*
3	*15*	*3 ±1*	*25 ±3*	*19 ±3*	*53 ±4*
4	150	7 ± 3	17 ± 3	13 ± 2	62 ± 2
6	20	5 ± 1	19 ± 2	16 ± 2	60 ± 2
7	50	4 ± 3	29 ± 6	28 ± 10	40 ± 6
8	50	8 ± 2	24 ± 5	14 ± 2	47 ± 5
9	50	16 ± 6	29 ± 8	10 ± 1	45 ± 1
10	50	13 ± 5	44 ± 6	26 ± 2	16 ± 1
13	*15*	*3 ±1*	*11 ±1*	*26 ±10*	*55 ±1*
14	20	6 ± 1	24 ± 5	15 ± 1	57 ± 8
15	15	2 ± 1	27 ± 3	14 ± 4	48 ± 11
16	20	4 ± 3	27 ± 1	22 ± 4	47 ± 6
17	20	4 ± 3	29 ± 1	16 ± 3	51 ± 3
18	20	4 ± 3	25 ± 3	16 ± 1	56 ± 1
19	150	5 ± 1	47 ± 6	15 ± 3	33 ± 2

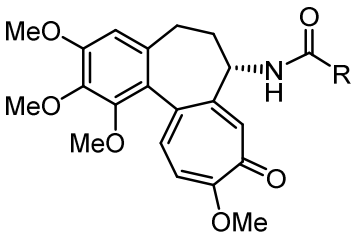

Colchicine R = Me (10 nM and 40 nM)

1	R = CH_2F	3 nM	**13**	R = 2-ClC_6H_4	1.5 nM
2	R = CH_2Cl	3 nM	**14**	R = 3-ClC_6H_4	1.5 nM
3	R = CH_2Br	10 nM	**15**	R = 4-ClC_6H_4	1.5 nM
4	R = CH_2I	10 nM	**16**	R = 2-BrC_6H_4	5 nM
9	R = 3-MeC_6H_4	2 nM	**17**	R = 3-BrC_6H_4	0.5 nM
12	R = 4-*t*BuPh	30 nM	**18**	R = 4-BrC_6H_4	9 nM

Figure 5.

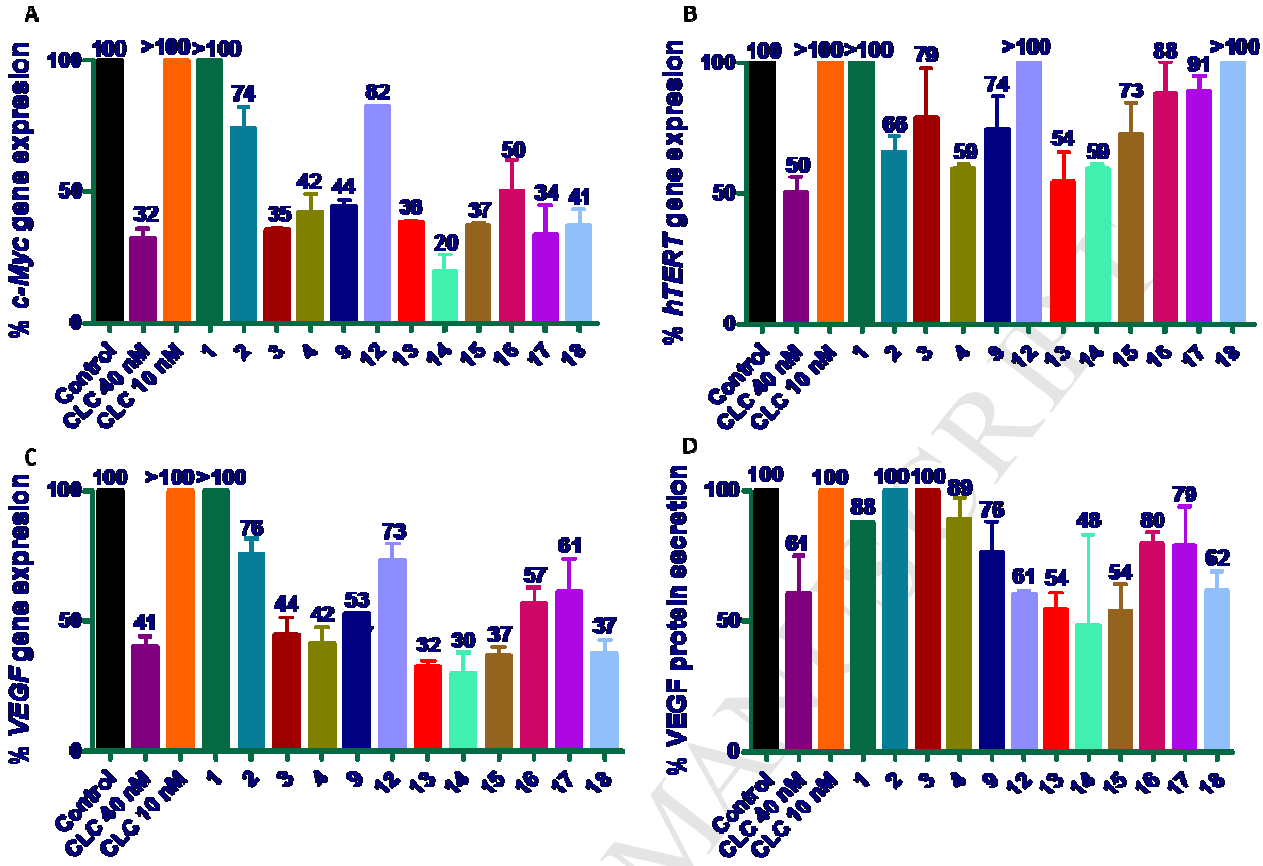

Figure 6.

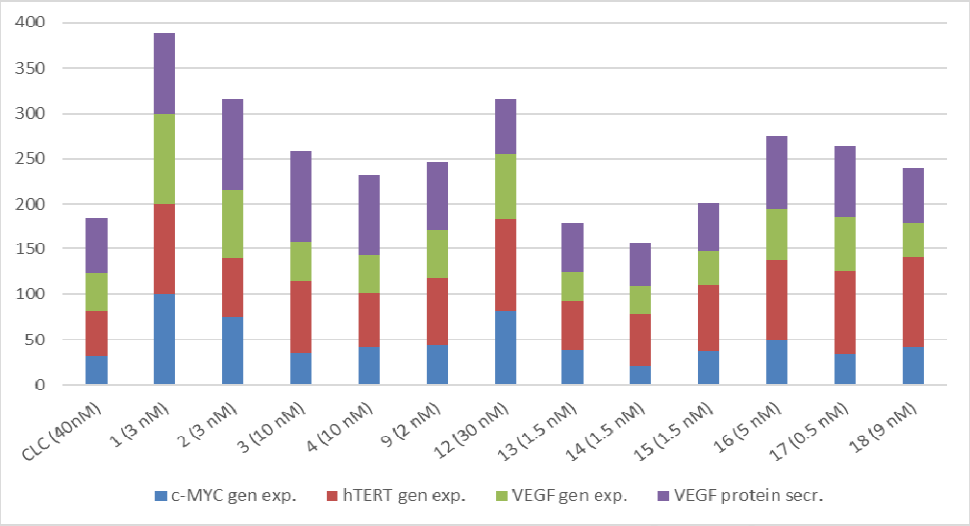

Figure 7.

Effects on tubulin polymerization and down-regulation of c-Myc, hTERT and VEGF genes by colchicine haloacetyl and haloaroyl derivatives

Ana Marzo-Mas, Eva Falomir, Juan Murga, Miguel Carda and J. Alberto Marco

Highlights

- Several *N*-acyl colchicine analogues have been synthesized.
- Their effect on the proliferation of several cell lines have been measured.
- Most compounds are able to inhibit in vitro tubulin polymerization.
- Some derivatives arrest cell cycle at G2/M phase at concentrations lower than colchicine.
- Some derivatives are able to downregulate some oncogene (VEGF, c-MYC and hTERT) expression at nontoxic concentrations.